Nuclear-structure and nuclear-astrophysics experiments at the superconducting electron accelerator ELBE

R. Schwengner[1], F. Dönau[1], M. Erhard[1], E. Grosse[1,2], A. R. Junghans[1], K. Kosev[1], C. Nair[1], N. Nankov[1,3], G. Rusev[1], K. D. Schilling[1], A. Wagner[1]

[1] *Institut für Kern- und Hadronenphysik, FZ Rossendorf, 01314 Dresden, Germany*
[2] *Institut für Kern- und Teilchenphysik, Technische Universität Dresden, 01062 Dresden, Germany*
[3] *Institute for Nuclear Research and Nuclear Energy, BAS, 1784 Sofia, Bulgaria*

- The bremsstrahlung facility
- Photon-scattering experiments
- Photoactivation experiments

Supported by the Deutsche Forschungsgemeinschaft

Bremsstrahlung facility at the ELBE accelerator

Accelerator parameters:

- Maximum electron energy: 20 MeV
- Maximum average current: 1 mA
- Micro-pulse rate: 26 or 260 MHz
- Reduction of 26 MHz by factors of 2 to 256
- Macro pulse of 0.1 to 36 ms length with periods of 40 ms to 1 s

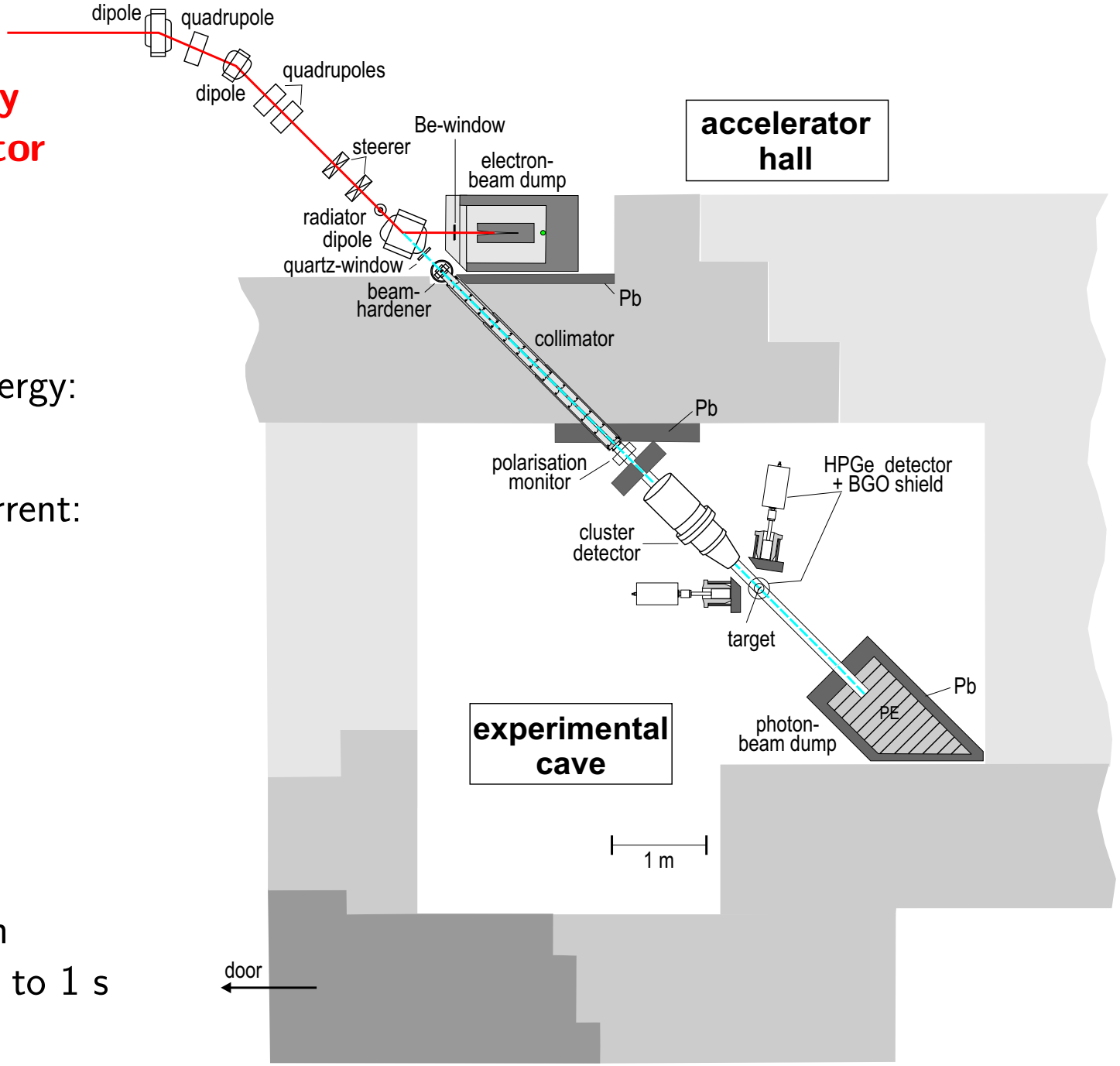

Electron-beam line

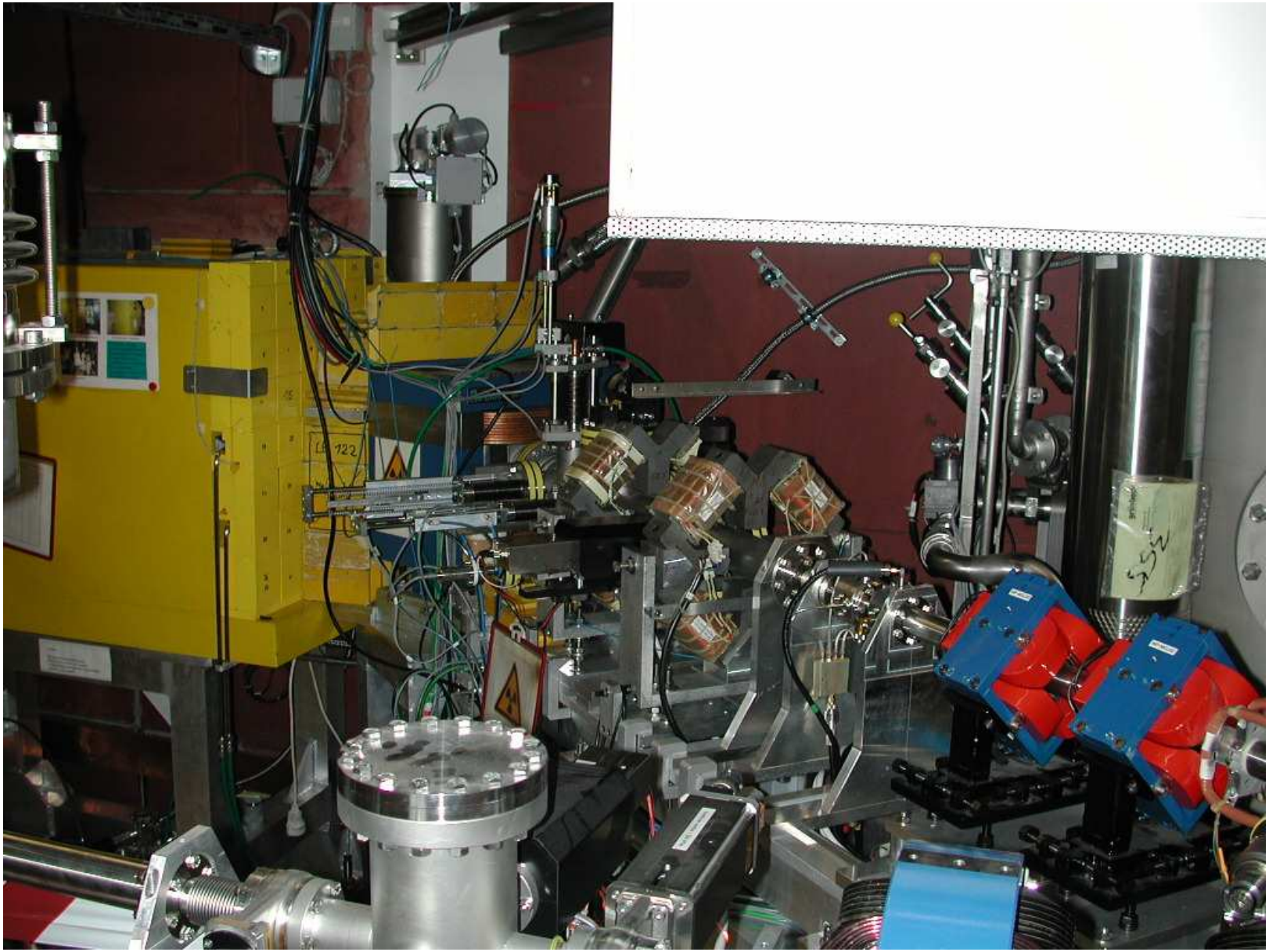

Simulation of the flux of photons passing the collimator

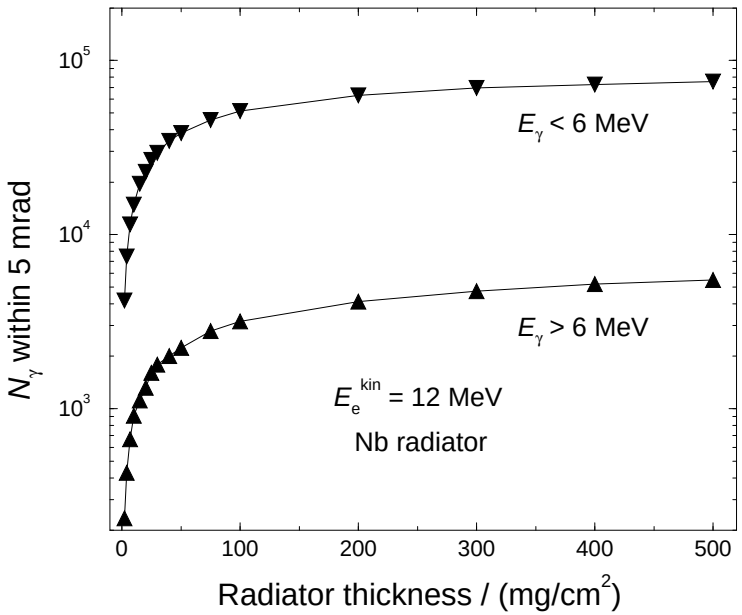

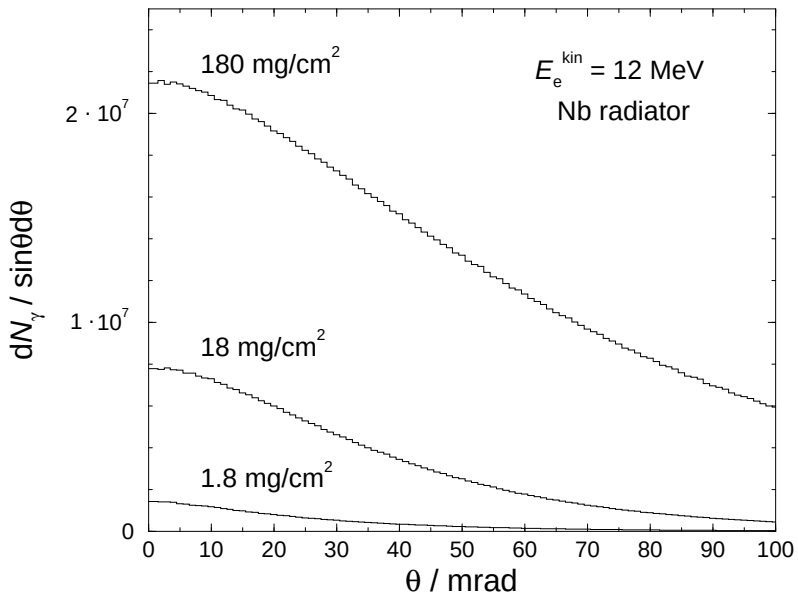

Simulations with GEANT4:

- Number of photons produced by 10^9 electrons of $E_e^{kin} = 12$ MeV in a cone with an opening angle of 5 mrad as a function of the niobium-radiator thickness.

- Number of photons produced by 10^9 electrons of $E_e^{kin} = 12$ MeV in niobium radiators of different thicknesses as a function of the angle between electron beam and photon.

Radiator

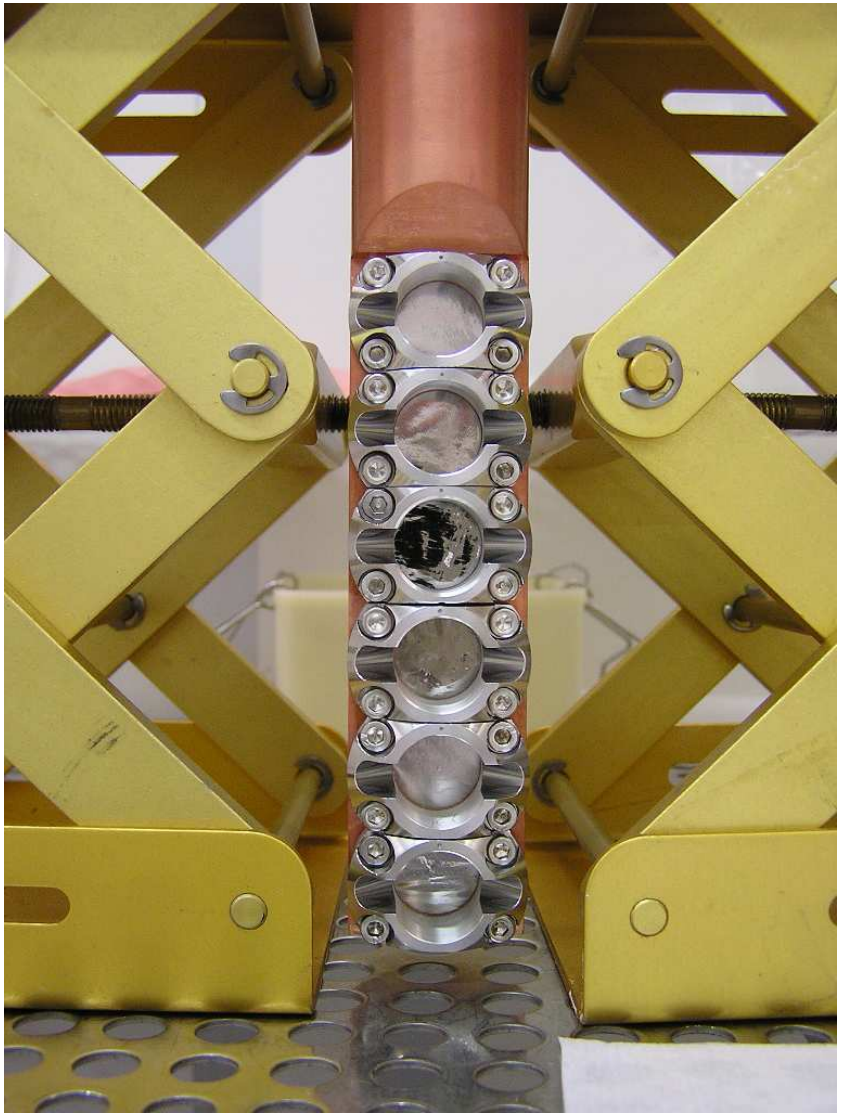

Niobium radiators:

- Six radiator foils of 16 mm diameter mounted on a water-cooled copper rod
- Thicknesses of 2, 3, 4, 5, 7 and 12.5 μm, corresponding to $2 \cdot 10^{-4}$ to 10^{-3} radiation lengths
- Radiator holder can be moved by a DC motor drive to select a radiator without breaking the vacuum

Detector setup

Beam dump

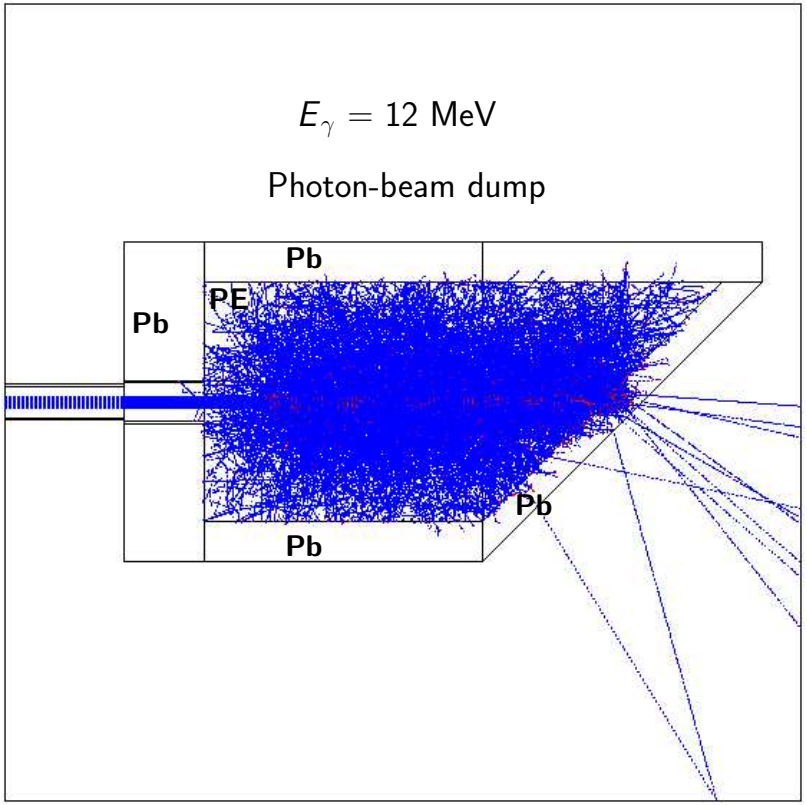

GEANT3 simulation with 1000 trajectories of 12 MeV photons.

About 0.3 % of the photons are scattered back towards the detectors.

Background measurements

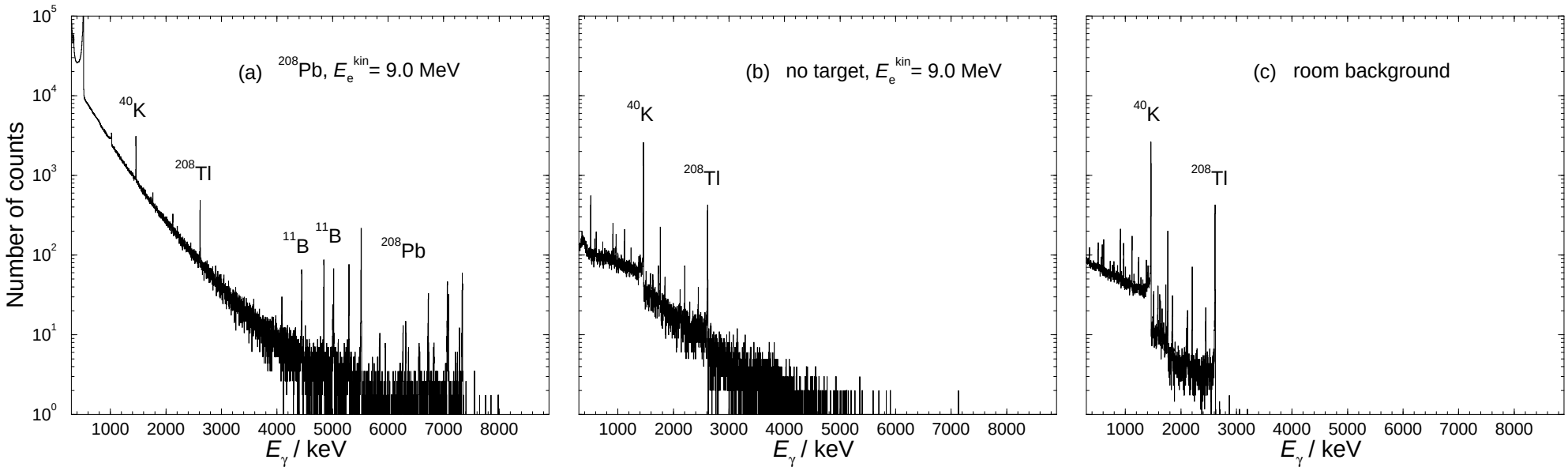

(a) Radiator thickness 4 μm, average beam current 480 μA, ^{208}Pb target of mass 1 g

(b) Radiator thickness 4 μm, average beam current 480 μA, no target

(c) Room background

- Measuring time 400 min

Measurement of the electron energy via photodisintegration of deuterons

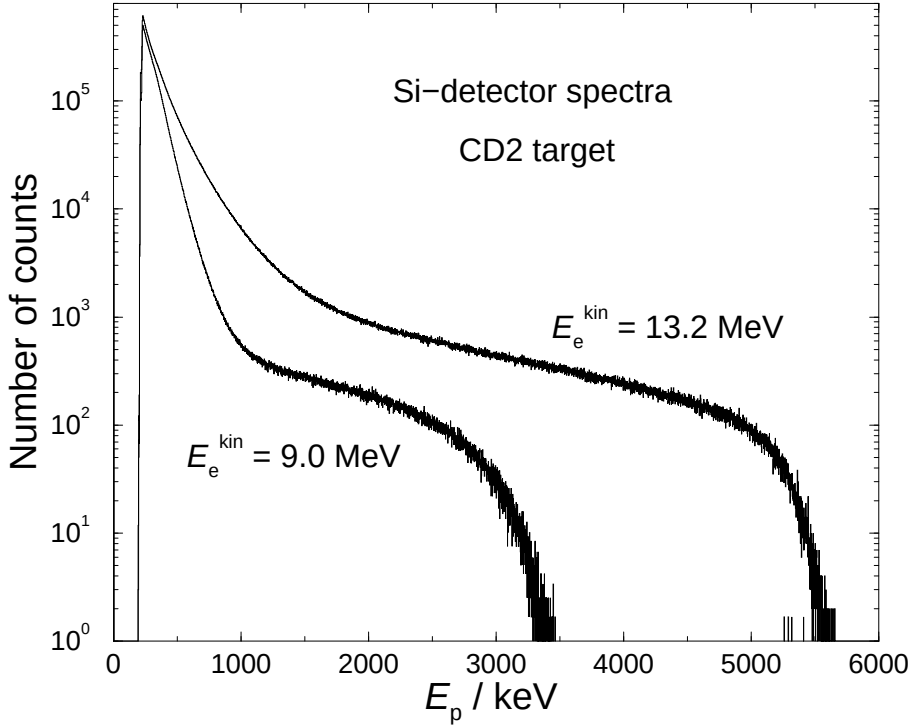

Spectra measured with Si detectors of 300 μm thickness during the irradiation of a deuterated polyethylene film with bremsstrahlung.

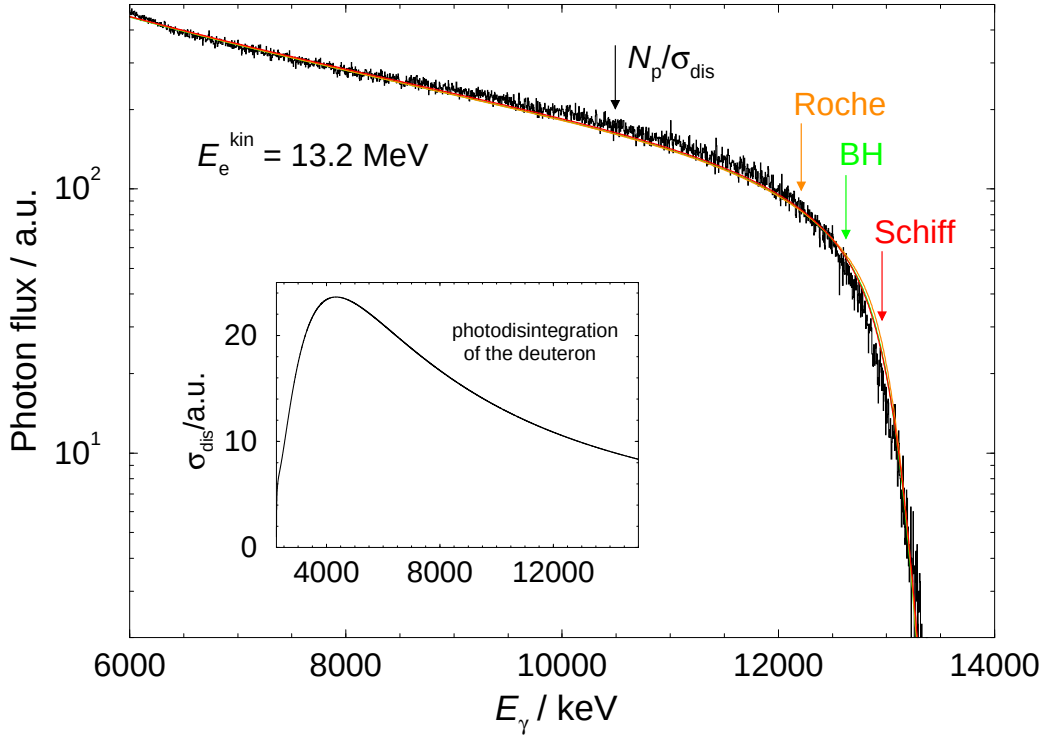

Spectrum of incident photons recalculated from the proton spectrum and the cross section for the disintegration of the deuteron.

σ_{dis}: H. Bethe, C. Longmire, Phys. Rev. 77 (1950) 647
Roche: G. Roche *et al.*, Phys. Rev. A 5 (1972) 2403
BH: H. Bethe, W. Heitler, Proc. Roy. Soc. A 146 (1934) 83
Schiff: L.I. Schiff, Phys. Rev. 83 (1951) 252

Production of linearly polarised off-axis bremsstrahlung

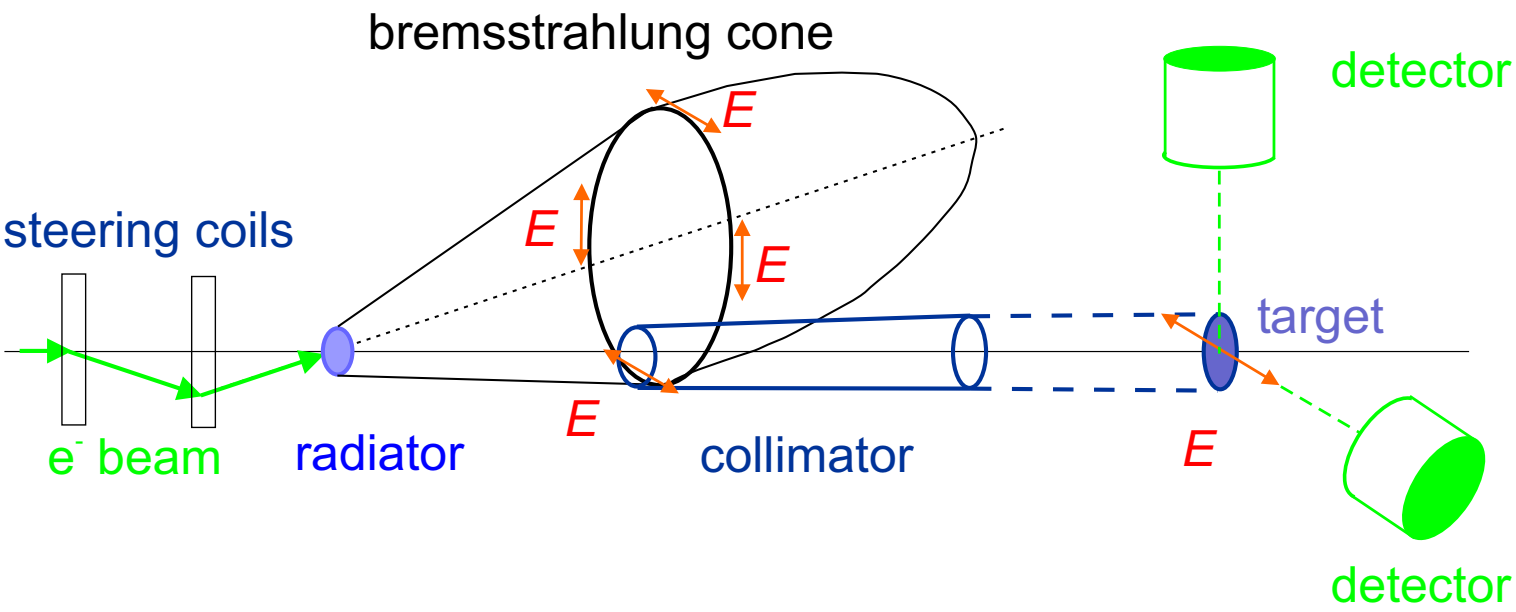

Measurement with polarised photons

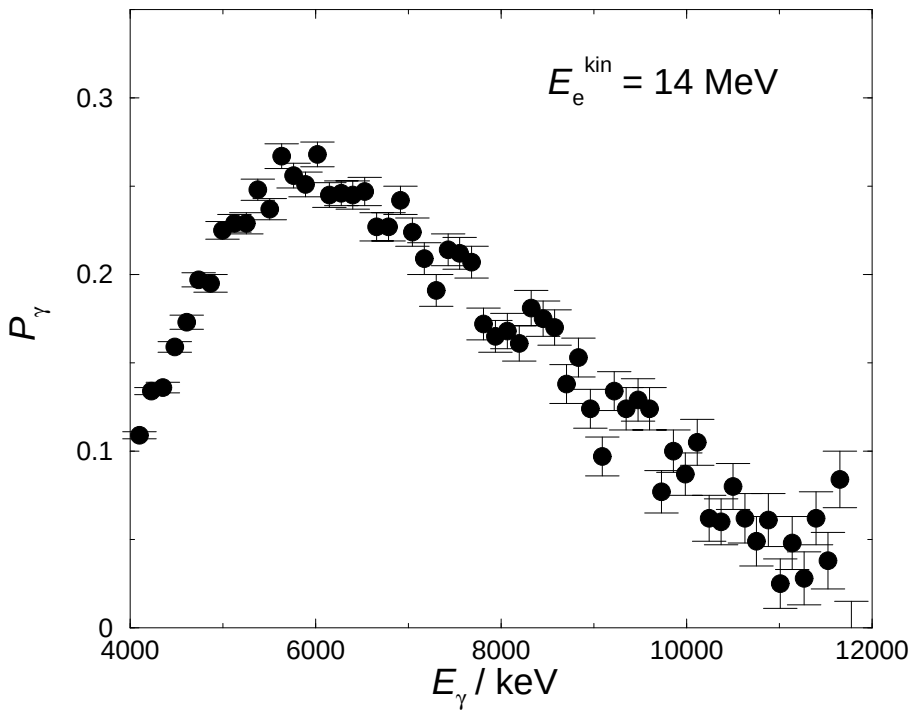

Degree of polarisation vs. photon energy as deduced from proton spectra.

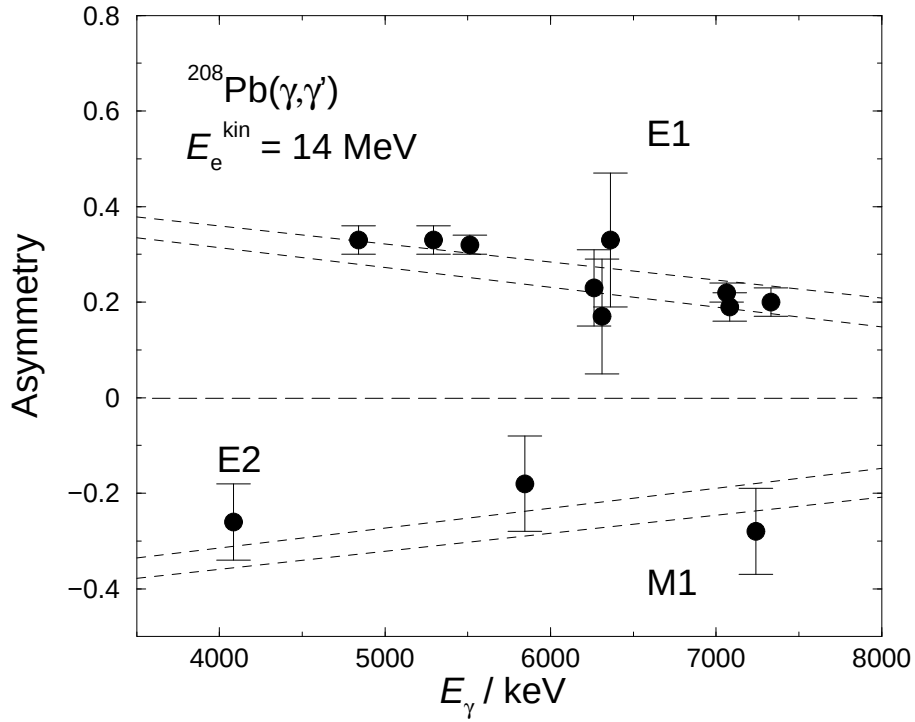

Experimental asymmetries of transitions in ^{208}Pb.

Photon scattering from ^{208}Pb

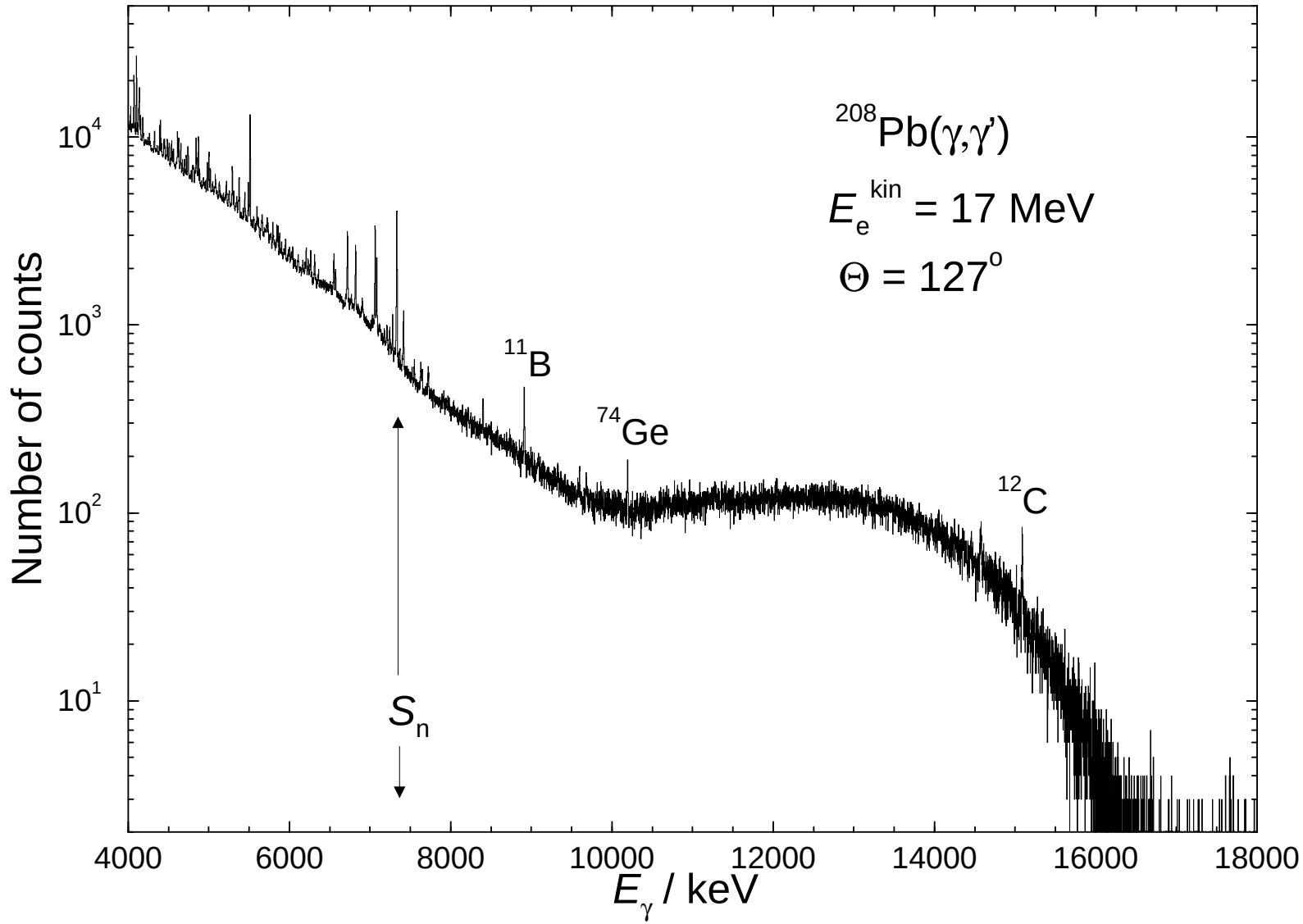

Nuclear resonance fluorescence

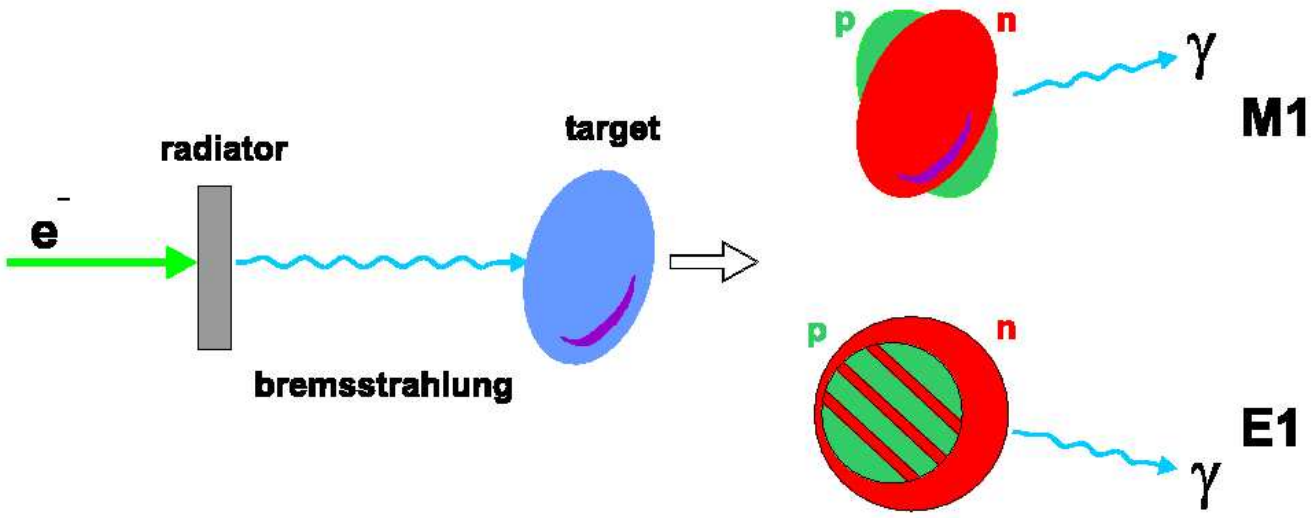

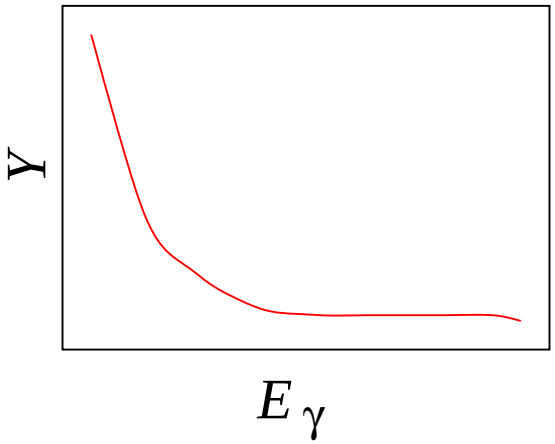

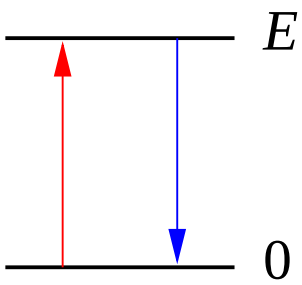

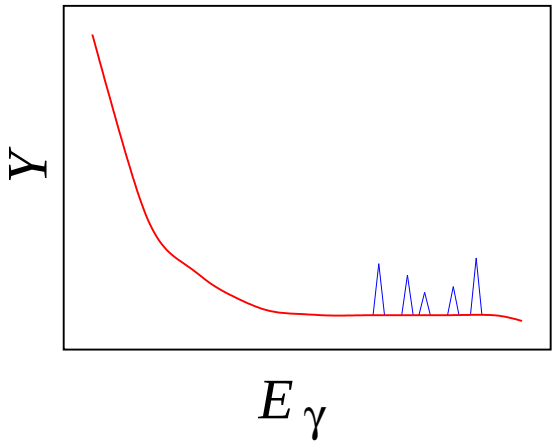

Photon scattering

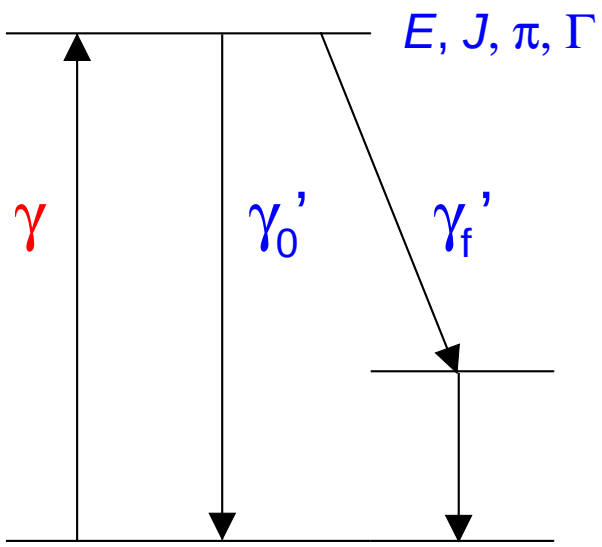

Experimental needs:

- Continuous photon spectrum of high intensity
  $\Rightarrow$ bremsstrahlung
- Variable end-point energy
  $\Rightarrow$ tunable electron energy

Experimental observables:

- Energy of the scattered photons $\longrightarrow E$
- Intensity of the scattered photons $\longrightarrow \Gamma$
- Angular distribution of the scattered photons $\longrightarrow J$
- Polarisation of the scattered photons $\longrightarrow \pi$
  $\Rightarrow$ Compton polarimeter ($E_\gamma < 5$ MeV)
  $\Rightarrow$ polarised bremsstrahlung for higher γ energies

Photon scattering

$$I_\gamma(E_\gamma, \Theta) = \sigma_s(E_i) \cdot \Phi_\gamma(E_i) \cdot \epsilon(E_\gamma) \cdot N_{at} \cdot \frac{d\Omega}{4\pi} \cdot W(E_\gamma, \Theta)$$

$$\frac{\sigma_s(E_i)}{\sigma_s(E_i^B)} = \frac{I_\gamma(E_\gamma, \Theta)}{I_\gamma(E_\gamma^B, \Theta)} \cdot \frac{\epsilon(E_\gamma^B)}{\epsilon(E_\gamma)} \cdot \frac{W(E_\gamma^B, \Theta)}{W(E_\gamma, \Theta)} \cdot \frac{N_{at}^B}{N_{at}} \cdot \frac{\Phi_\gamma(E_i^B)}{\Phi_\gamma(E_i)}$$

$$\sigma_s = g \left(\frac{\pi\hbar c}{E_i}\right)^2 \frac{\Gamma_0 \Gamma_f}{\Gamma}; \quad g = \frac{2J_i + 1}{2J_0 + 1}; \quad \Gamma = \frac{\hbar}{\tau}$$

$$B(E1)\uparrow = g\, B(E1)\downarrow = 2.866 \cdot 10^{-3} \cdot \frac{\Gamma_0/\mathrm{meV}}{(E_\gamma/\mathrm{MeV})^3}\ e^2\mathrm{fm}^2$$

$$B(M1)\uparrow = g\, B(M1)\downarrow = 0.2598 \cdot \frac{\Gamma_0/\mathrm{meV}}{(E_\gamma/\mathrm{MeV})^3}\ \mu_N^2$$

$$B(E2)\uparrow = g\, B(E2)\downarrow = 6201 \cdot \frac{\Gamma_0/\mathrm{meV}}{(E_\gamma/\mathrm{MeV})^5}\ e^2\mathrm{fm}^4$$

Nuclides under investigation in photon-scattering experiments

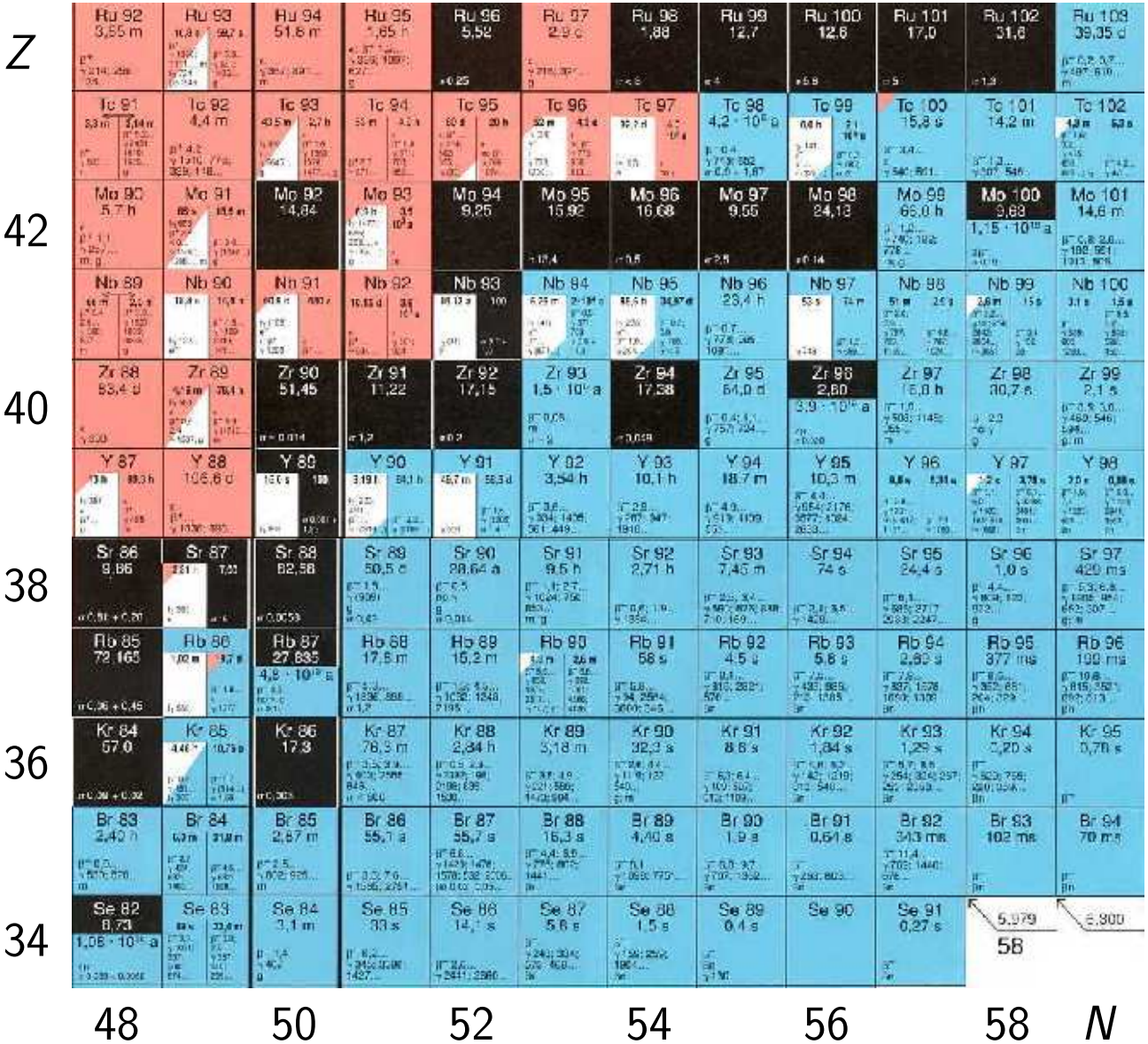

nuclide	S_n MeV	E_e^{kin} MeV
^{92}Mo	12.7	6.0, 13.2
^{98}Mo	8.6	13.2 3.3[a], 3.8[a]
^{100}Mo	8.3	7.8, 13.2 3.2[a], 3.4[a], 3.8[a]
^{88}Sr	11.1	9.0, 13.2 6.8[b]
^{90}Zr	12.0	7.0, 9.0

[a] Dynamitron experiment, PRL 95 (2005) 062501

[b] S-Dalinac experiment, PRC 70 (2004) 064307

M1 strength in even-even Mo isotopes up to 4 MeV

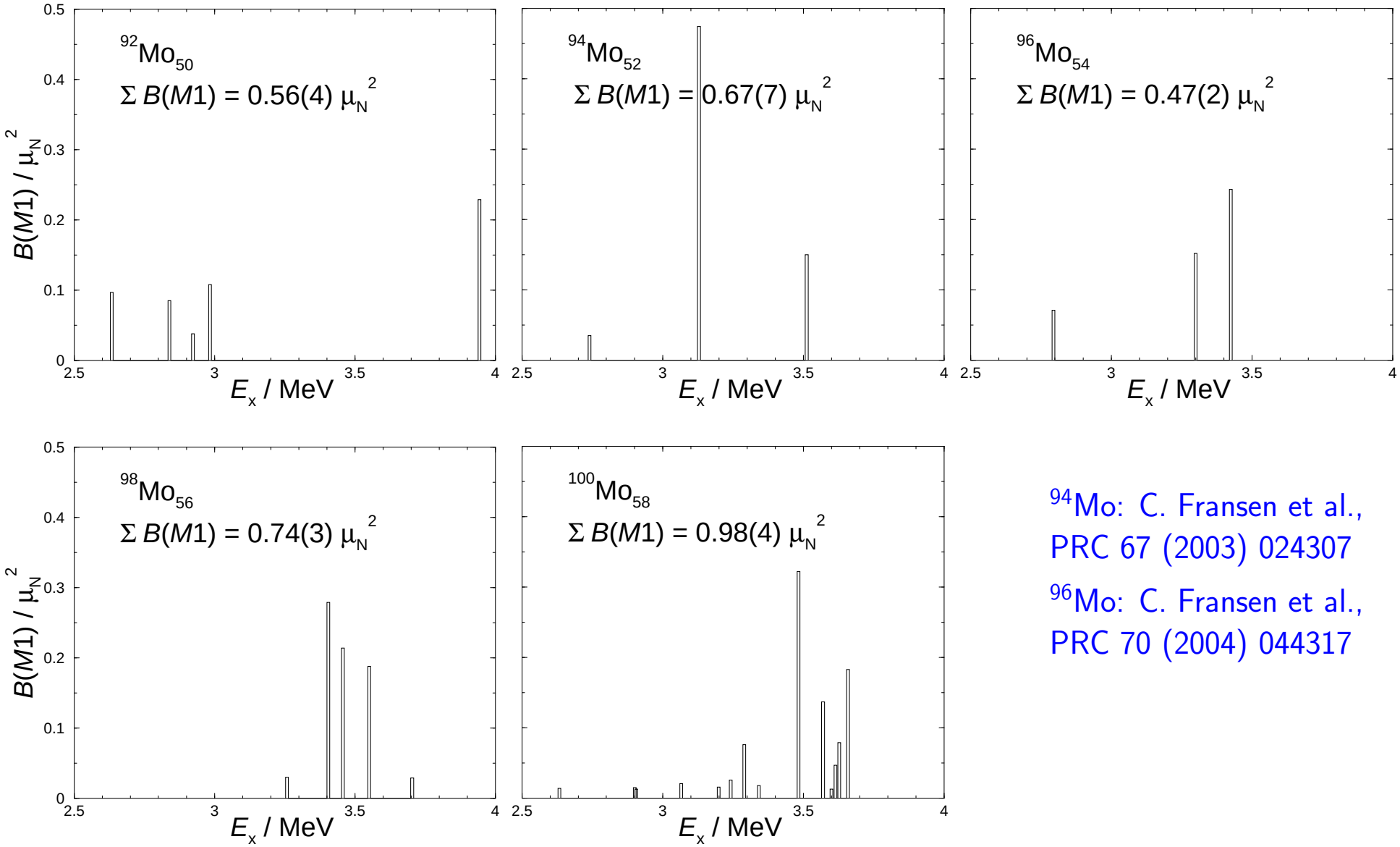

^{94}Mo: C. Fransen et al., PRC 67 (2003) 024307

^{96}Mo: C. Fransen et al., PRC 70 (2004) 044317

Deformation of even-even Mo isotopes

Total energy as a function of the quadrupole deformation ε_2 and the triaxiality γ:

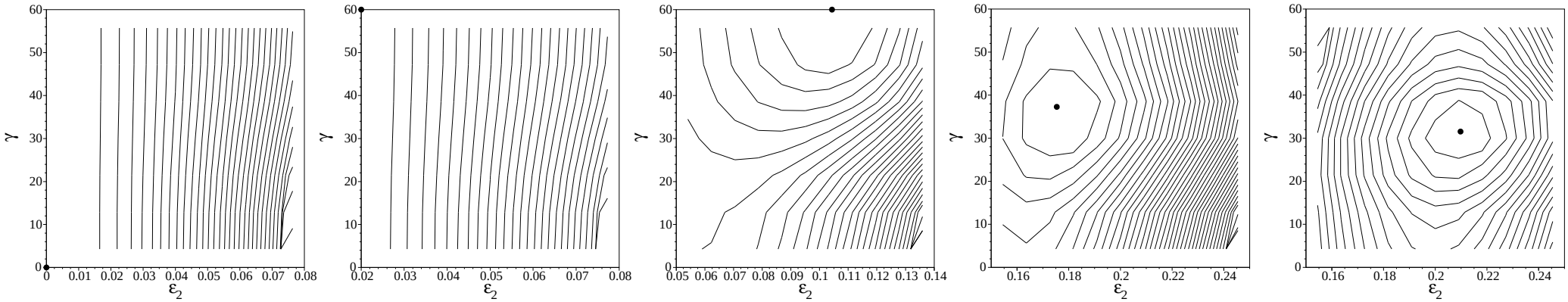

$^{92}Mo_{50}$	$^{94}Mo_{52}$	$^{96}Mo_{54}$	$^{98}Mo_{56}$	$^{100}Mo_{58}$
$\varepsilon_2 = 0.0$	$\varepsilon_2 = 0.02$	$\varepsilon_2 = 0.10$	$\varepsilon_2 = 0.18$	$\varepsilon_2 = 0.21$
		$\gamma = 60^\circ$	$\gamma = 37^\circ$	$\gamma = 32^\circ$

TAC model with shell-correction method

S. Frauendorf, NPA 557 (1993) 259c, NPA 667 (2000) 115

M1 strength in even-even Mo isotopes up to 4 MeV

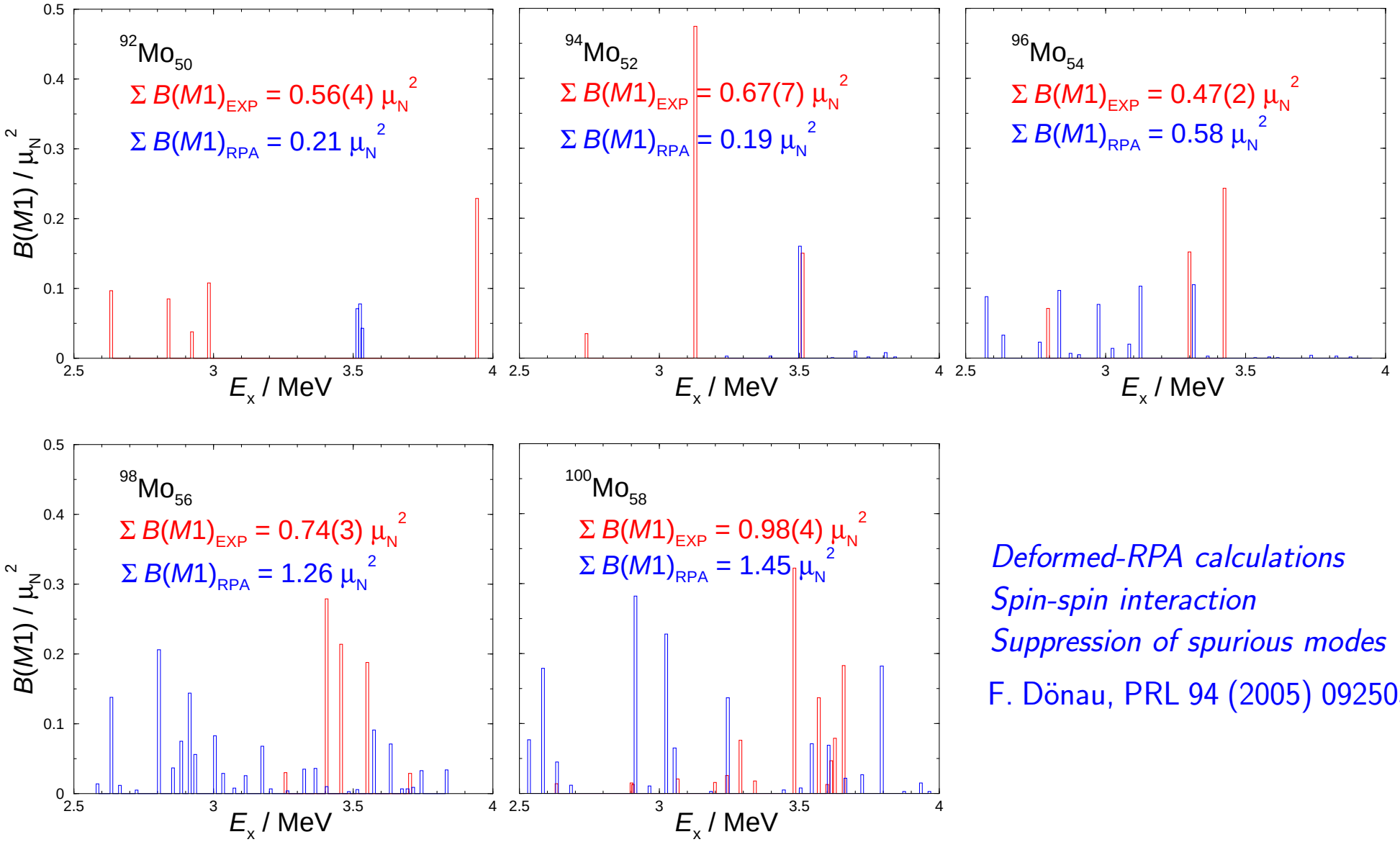

Deformed-RPA calculations
Spin-spin interaction
Suppression of spurious modes

F. Dönau, PRL 94 (2005) 092503

Photon scattering from ^{92}Mo, ^{98}Mo and ^{100}Mo

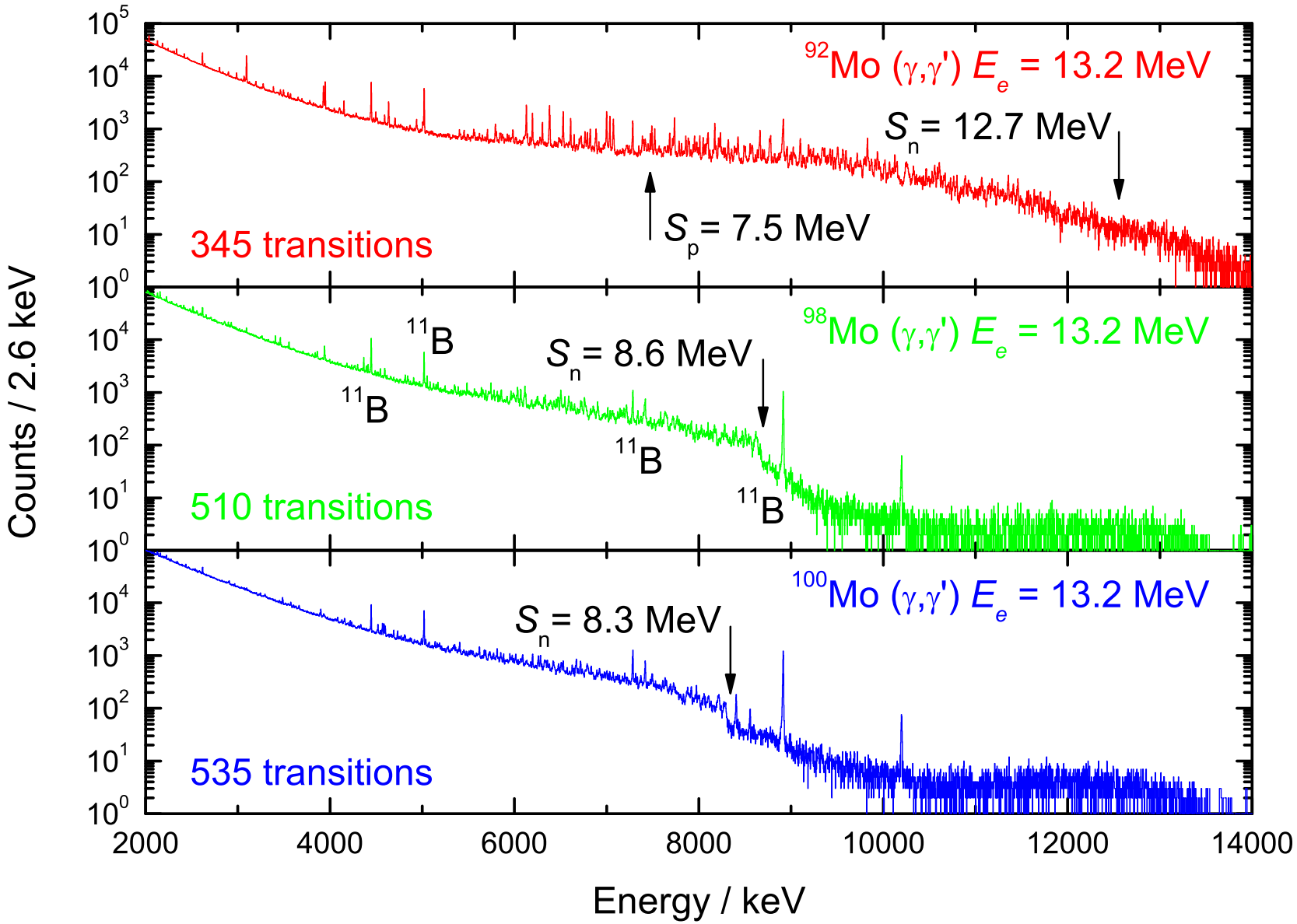

Detection limits

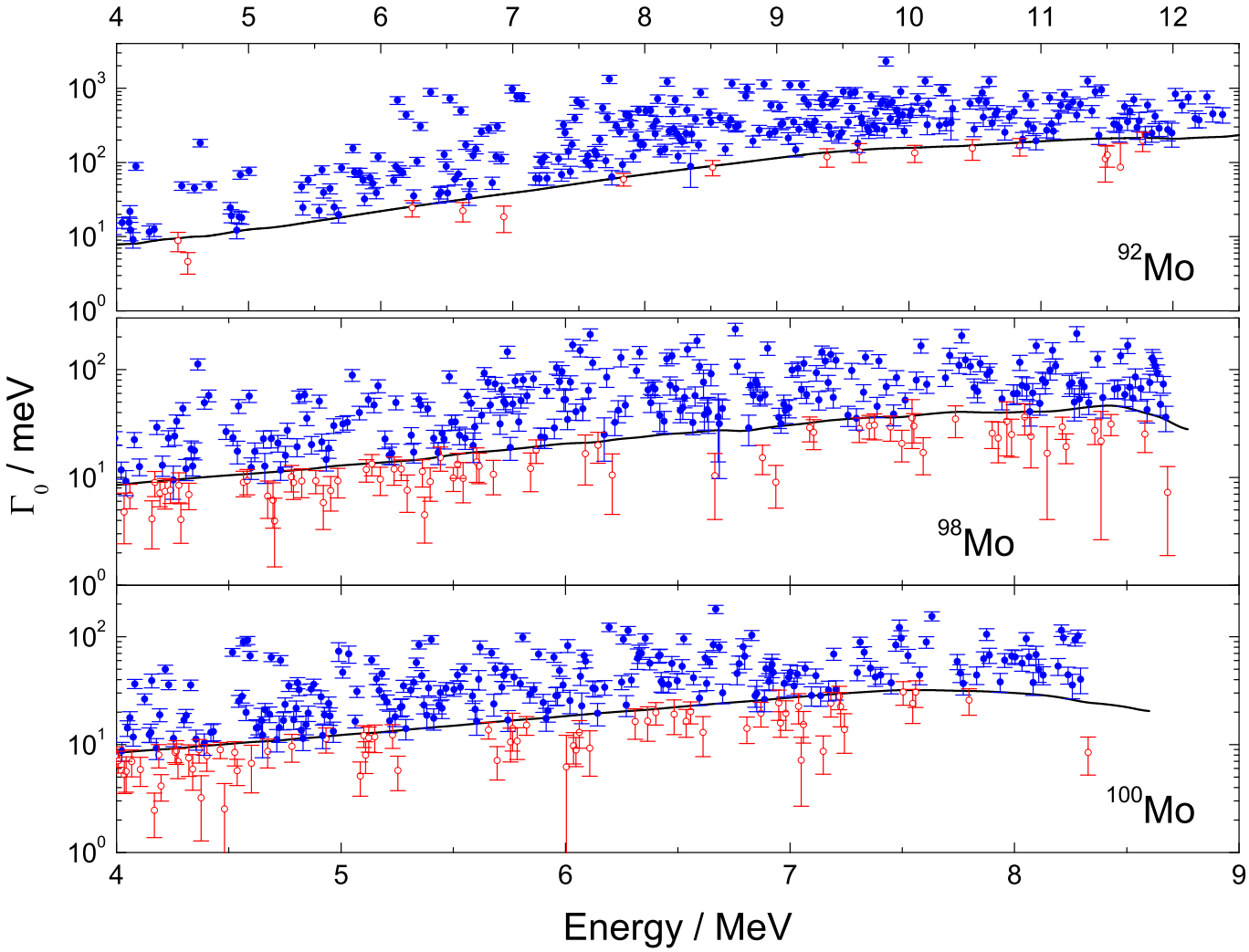

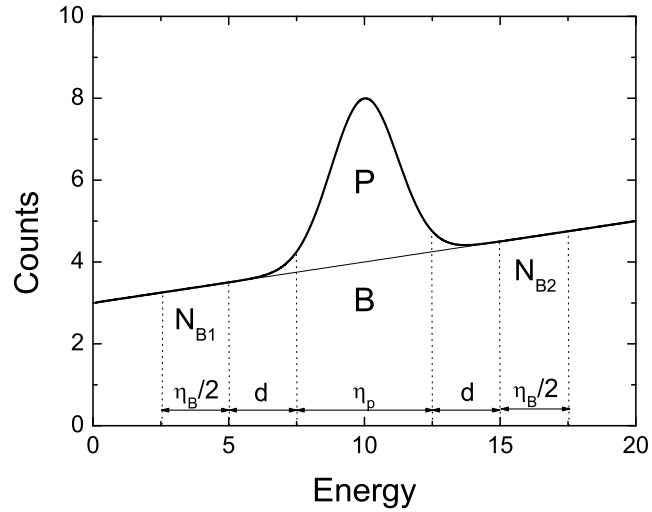

$$p_{DL} = 3\sqrt{(1+\frac{\eta_P}{\eta_B})B}$$

R. Jenkins, R.W. Gould, D. Gedcke, *Quantitative X-Ray Spectrometry*, Marcel Dekker, New York, 1981

Angular distributions of transitions in ^{92}Mo, ^{98}Mo and ^{100}Mo

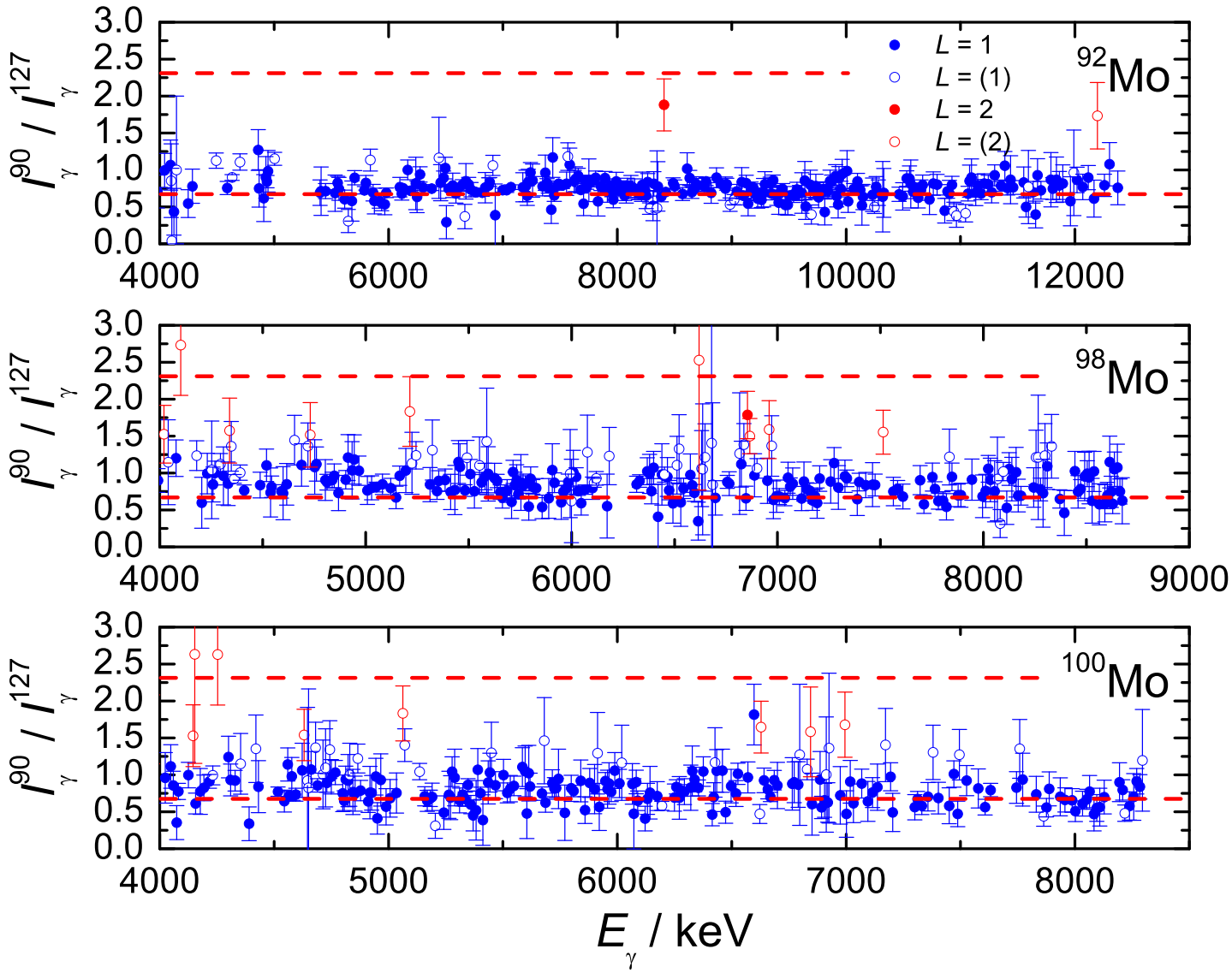

Expected values:

$L = 1$:

$I_\gamma(90°)/I_\gamma(127°) = 0.73$

$L = 2$:

$I_\gamma(90°)/I_\gamma(127°) = 2.28$

E1 strength in ^{92}Mo, ^{98}Mo and ^{100}Mo

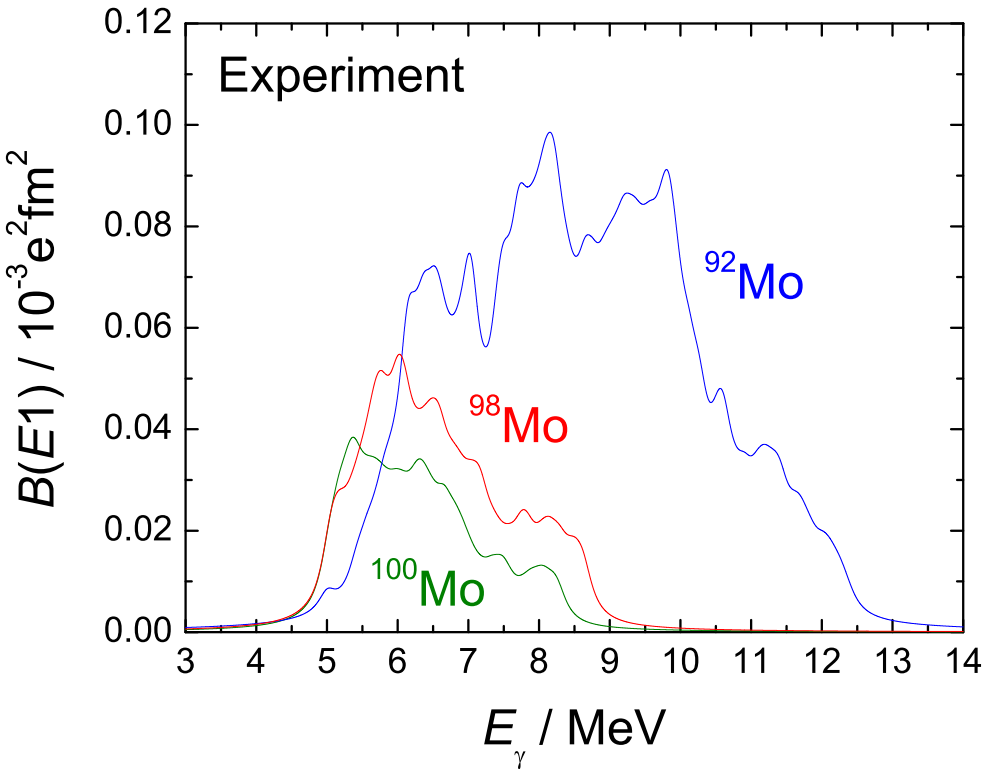

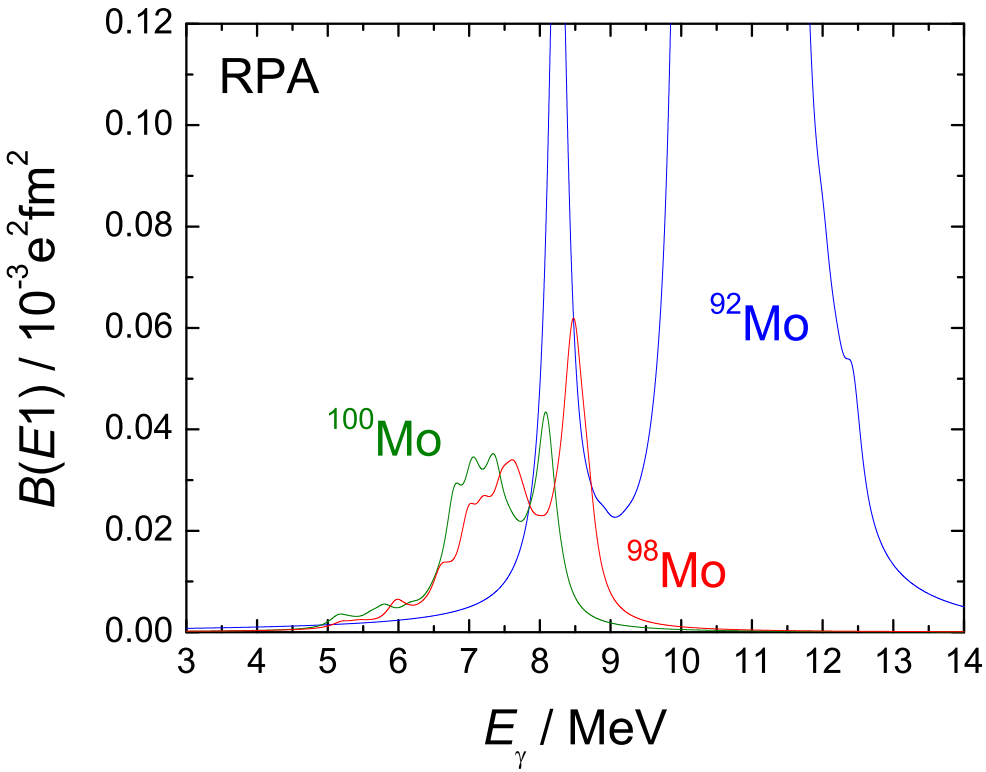

The summed $B(E1)$ strength *decreases* with increasing N/Z.

E1 strength in even-even Mo isotopes and in even-even N = 50 isotones

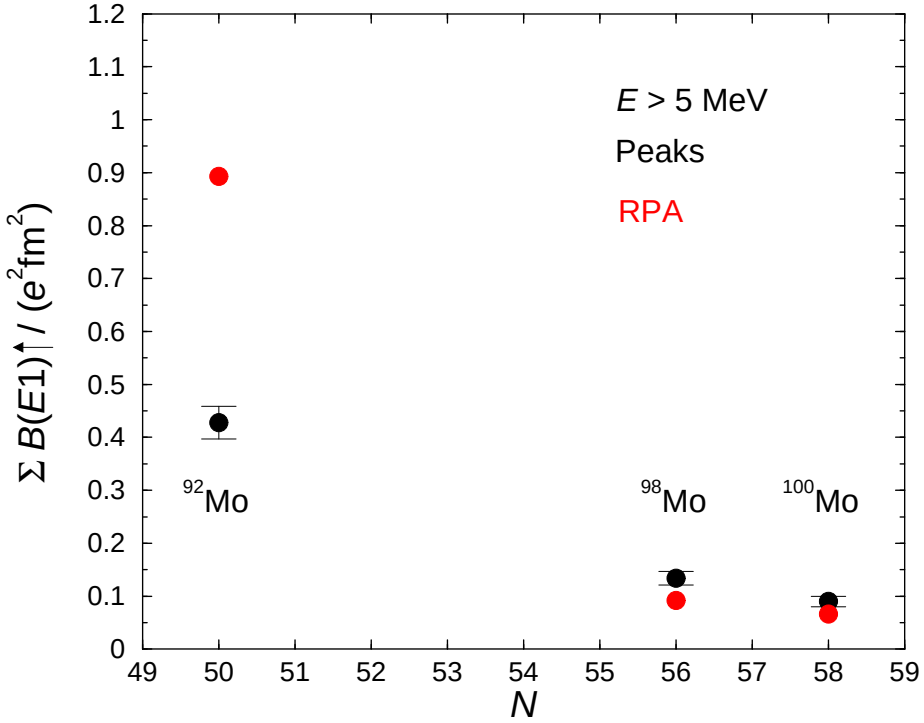

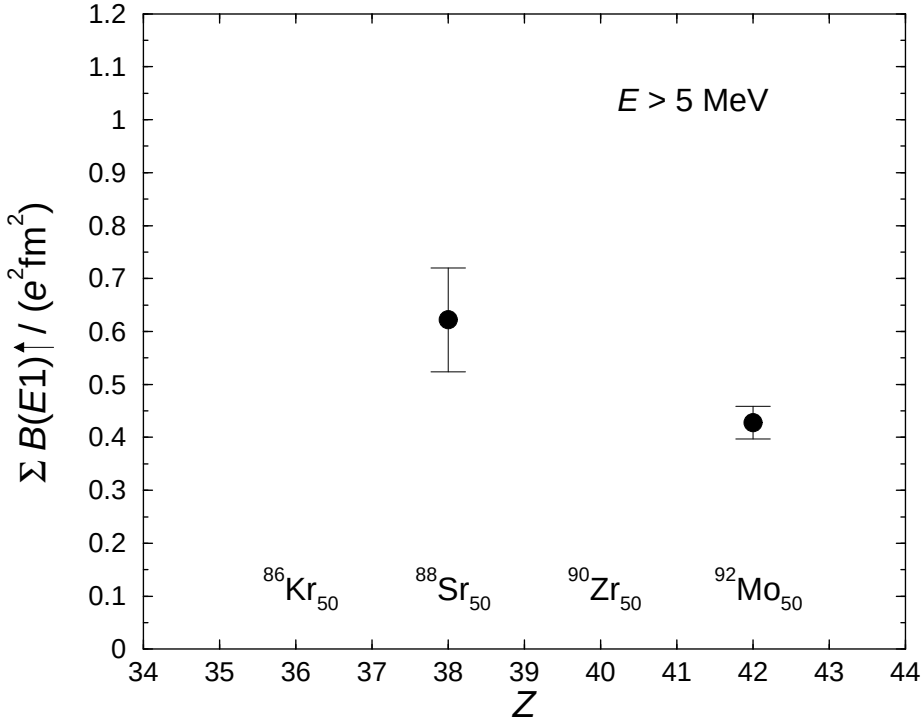

The summed $B(E1)$ strength *decreases* with increasing N/Z.

The summed $B(E1)$ strength *increases* with increasing N/Z.

Unresolved strength in the continuum

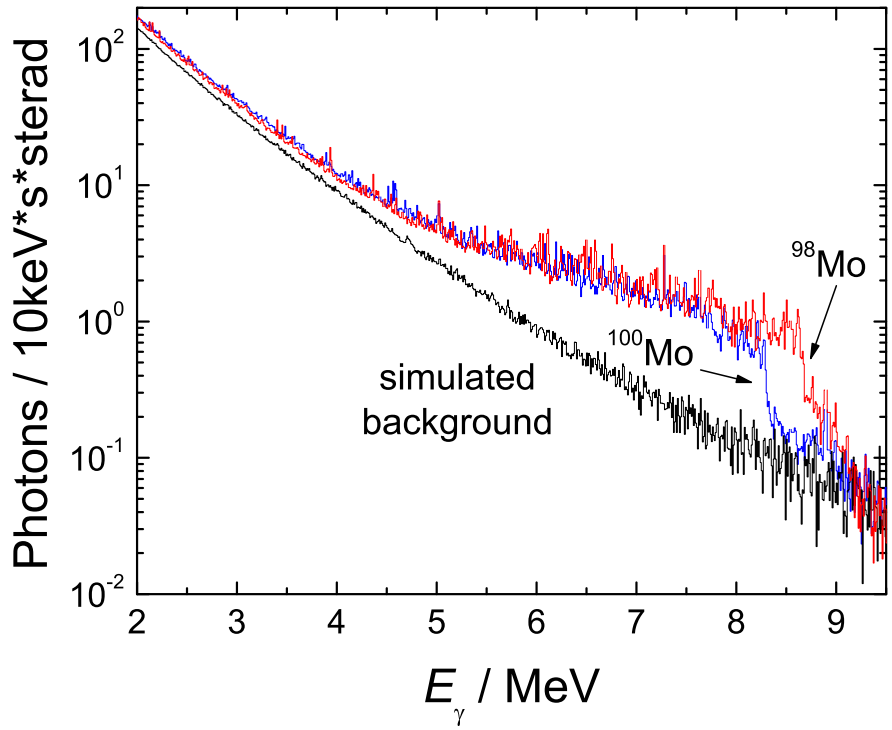

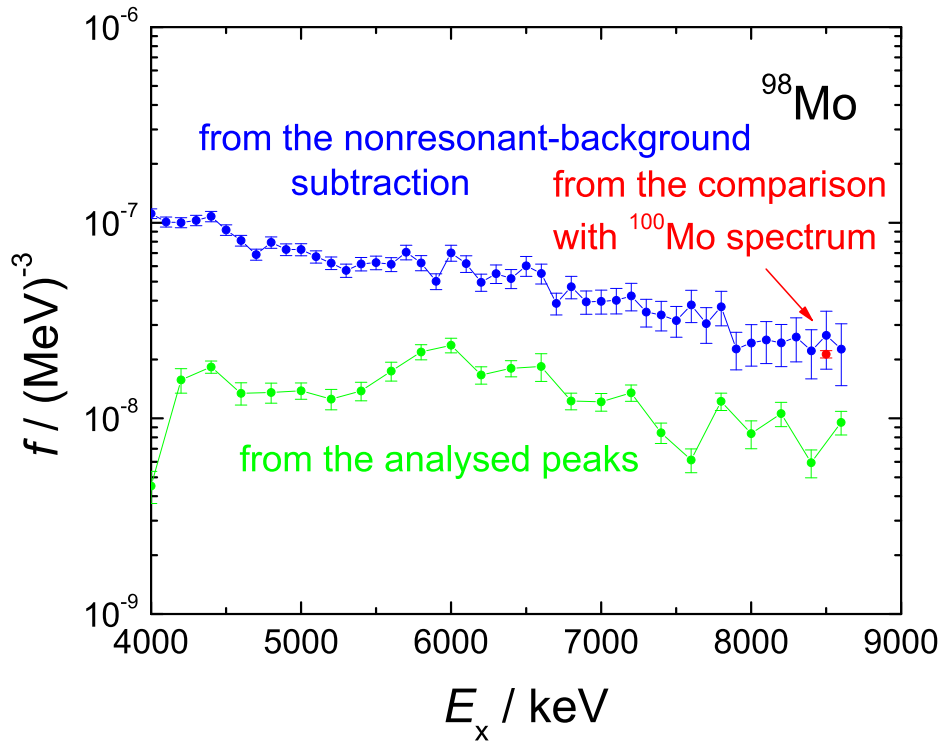

$$f_L(E) = \frac{1}{\Delta} \sum_{\Delta} \frac{\Gamma_0}{E^3}$$

E1 strength in even-even Mo isotopes and in even-even N = 50 isotones

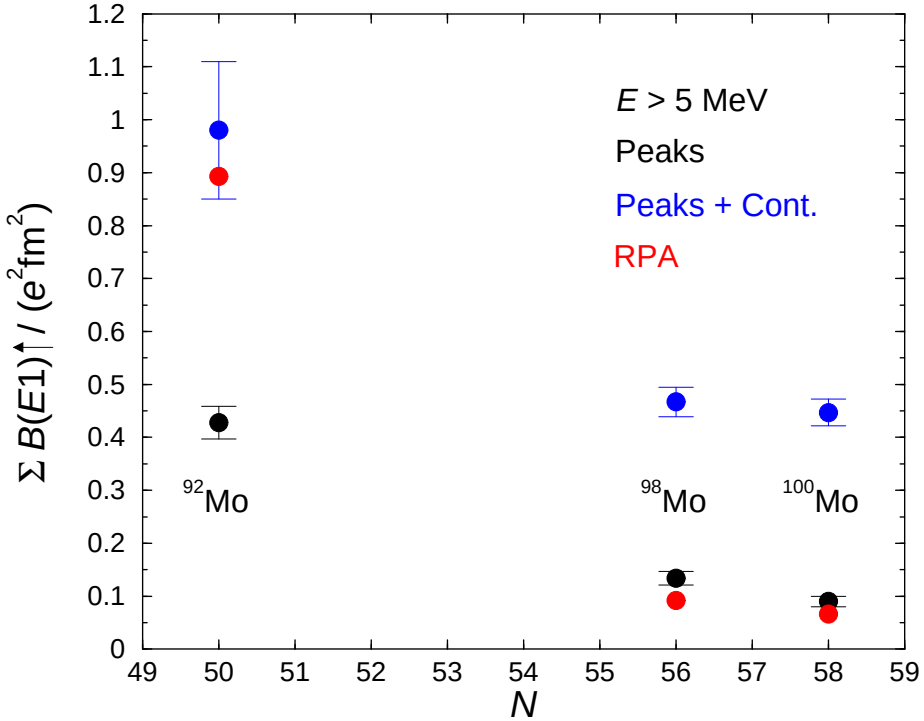

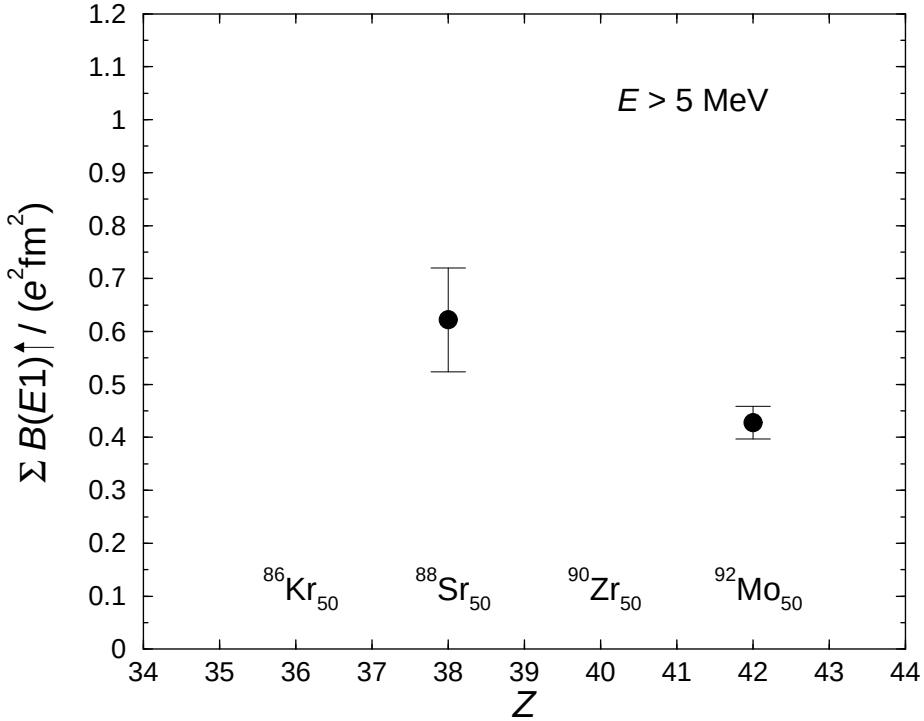

The summed $B(E1)$ strength *decreases* with increasing N/Z.

The summed $B(E1)$ strength *increases* with increasing N/Z.

Statistical analysis

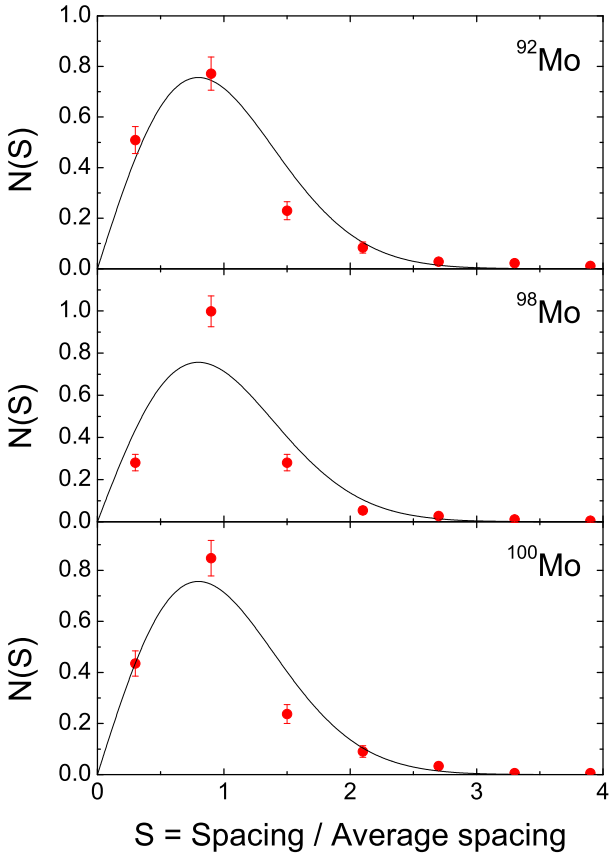

Level-spacing distributions for levels with $E > 4$ MeV. The drawn lines represent Wigner distributions.

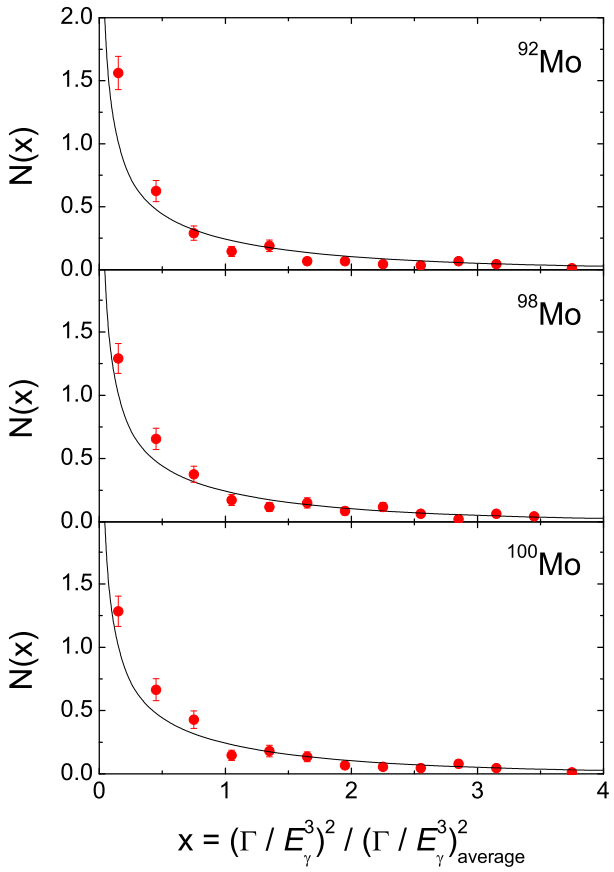

Distributions of reduced level widths for levels with $E > 4$ MeV. The drawn lines represent Porter-Thomas distributions.

Problem of feeding and branching

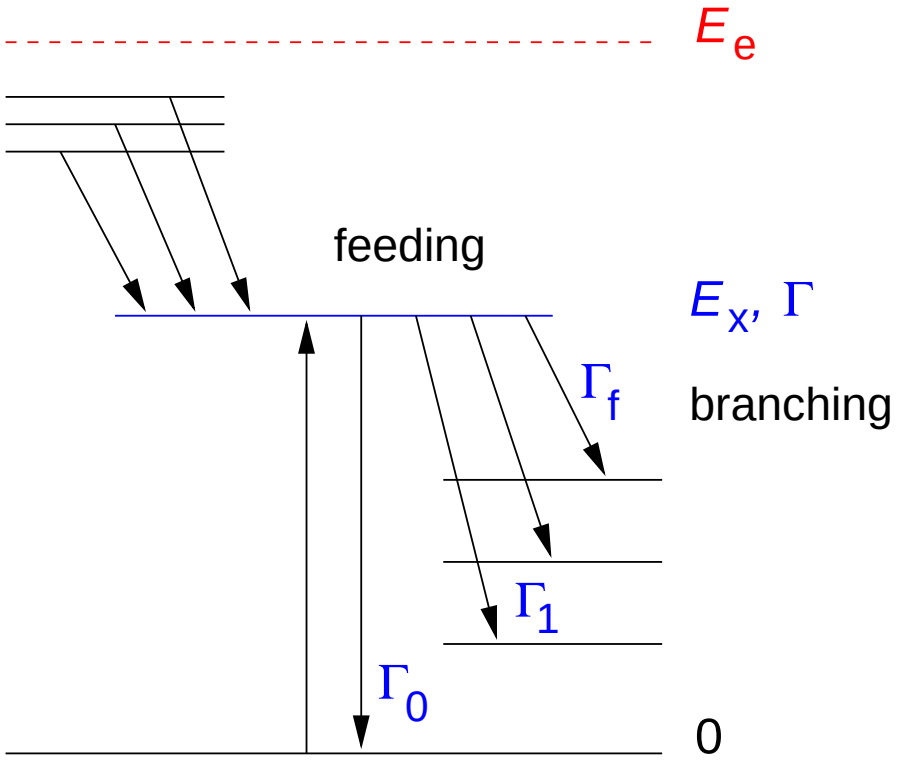

Feeding from high-lying states:

$\longrightarrow$ Determination of the widths Γ from measurements at various energies

Branching to low-lying states:

$\longrightarrow$ Correction of the strength distribution f_L by using statistical methods:

The branching ratios Γ_f/Γ are calculated by means of Monte Carlo simulations of the decays. Intensities are corrected with calculated branching ratios.

A level scheme of $J = 1$ and 2 states is constructed with a model using the Wigner level-spacing distribution and level densities given by the backshifted Fermi-gas model. The partial decay width is given by:

$$\Gamma_{if} = \sum_{X,L} y_{XL}^2 (E_i - E_f)^{2L+1} \frac{f_{XL}(E_i - E_f)}{\rho(E_i, J_i^\pi)}$$

Reconstructed dipole-strength distributions in ^{92}Mo, ^{98}Mo and ^{100}Mo

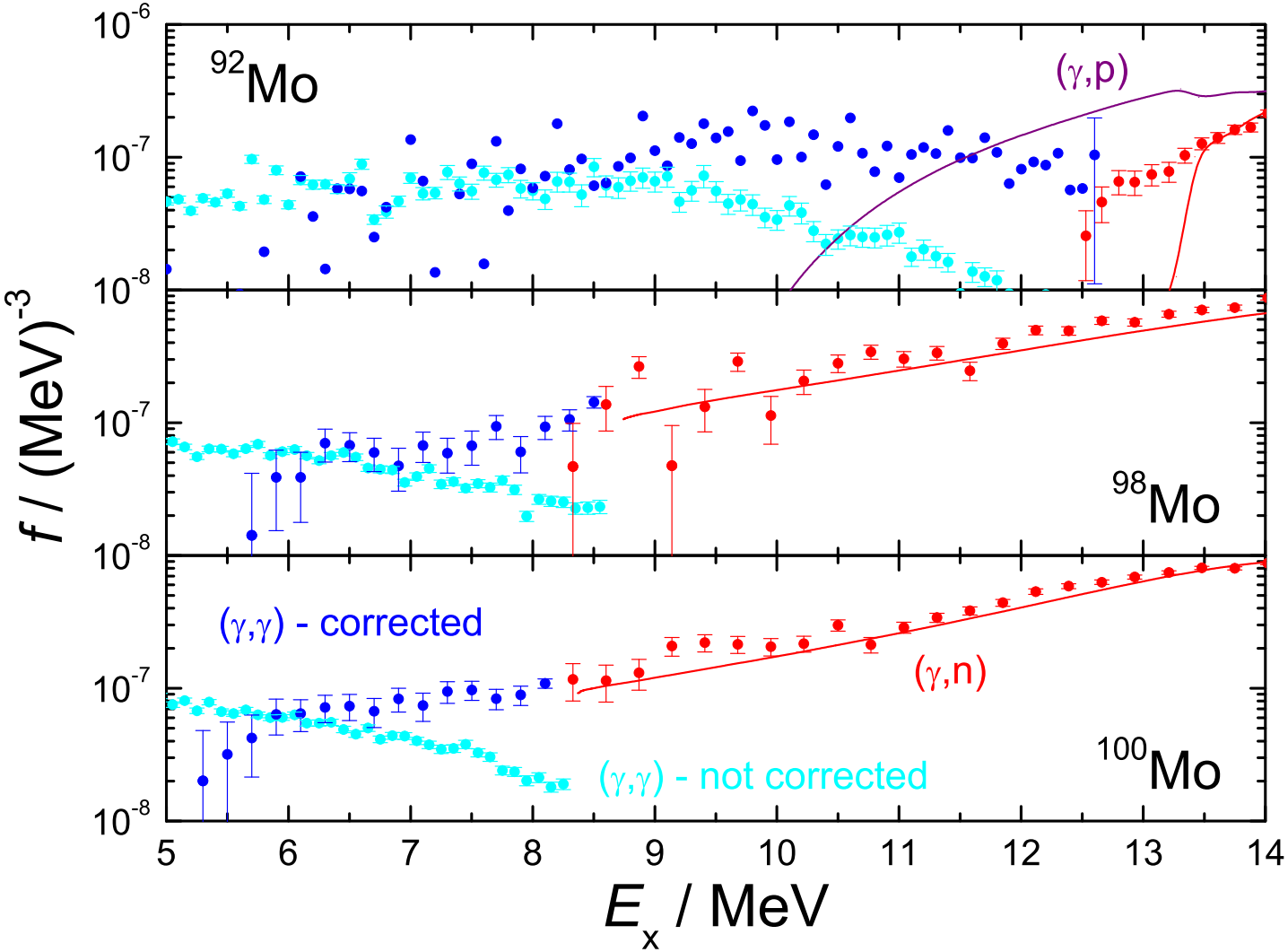

(γ, n) - experiment:
H. Beil et al.,
NPA 227 (1974) 427

(γ, n) and (γ, p) - theory:
T. Rauscher and
F.-K. Thielemann,
ADNDT 88 (2004) 1

$$E < S_n: \quad f_L(E) = \frac{1}{3(\pi\hbar c)^2 \Delta} \sum_i \frac{\int \sigma_i^{\mathrm{corr}} dE}{E_i} \qquad E > S_n: \quad f_L(E) = \frac{1}{3(\pi\hbar c)^2} \left\langle \frac{\sigma_{\gamma,n}(E)}{E} \right\rangle$$

Accumulative E1 strength

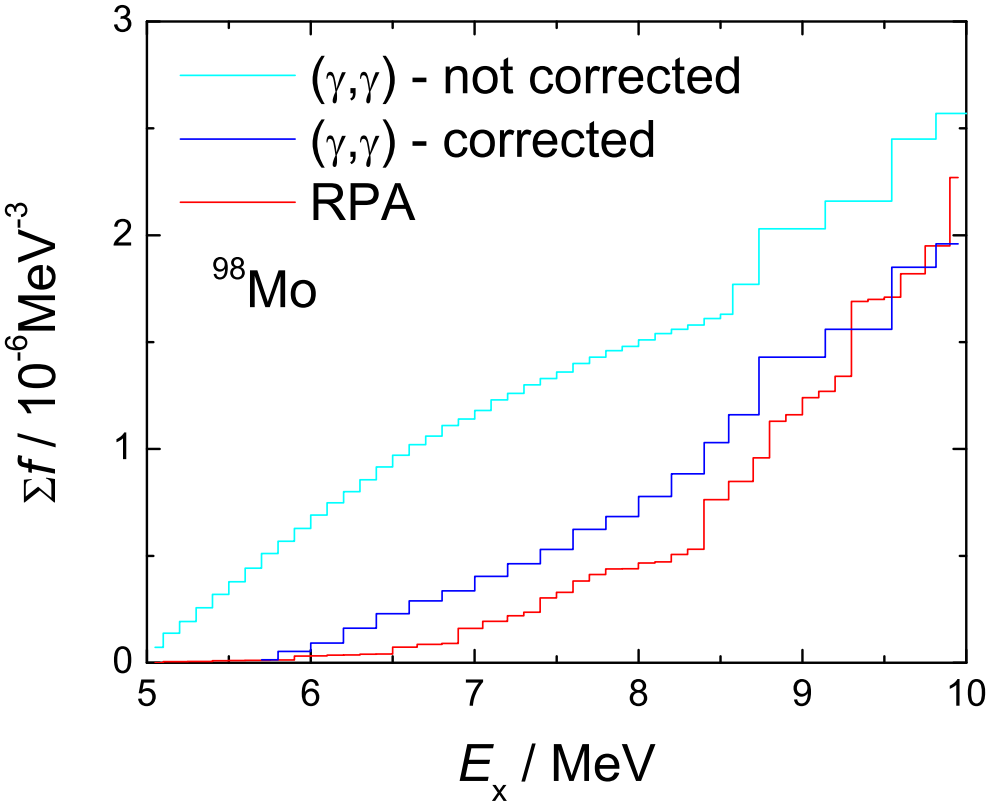

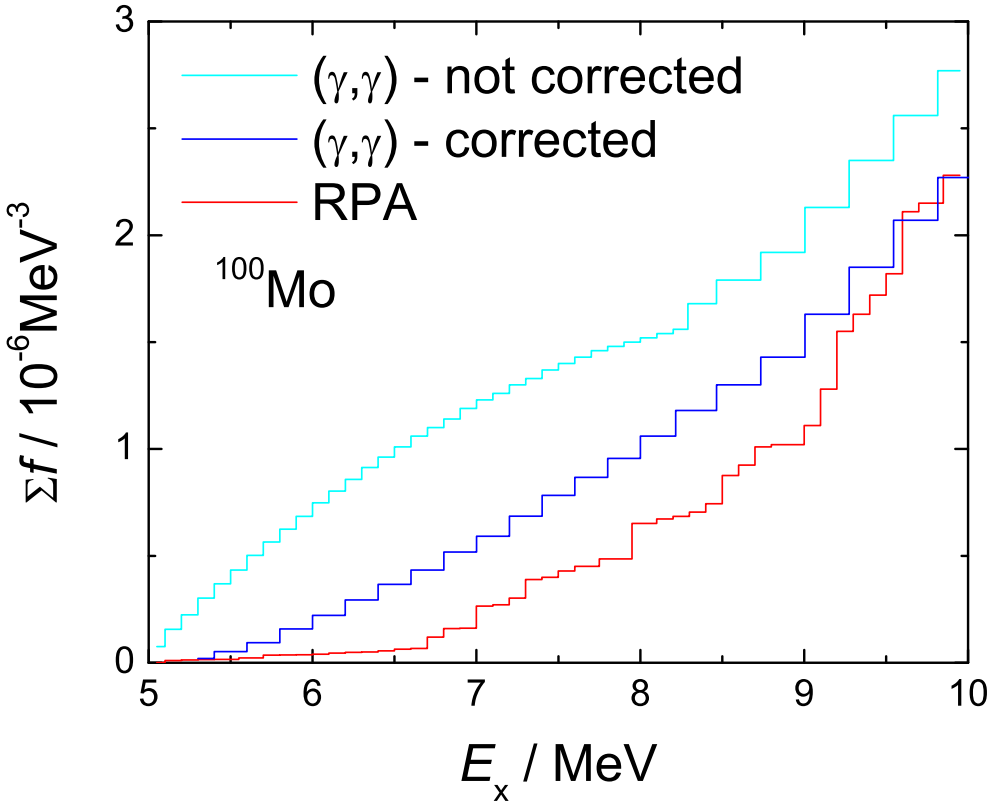

Photon scattering from ^{88}Sr and ^{90}Zr

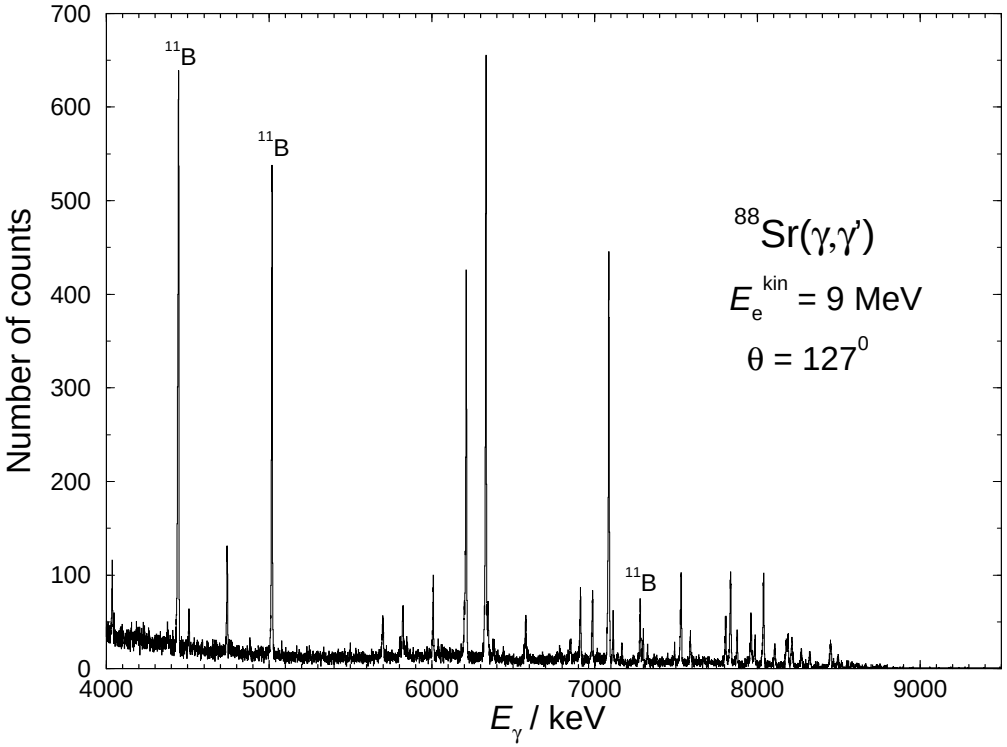

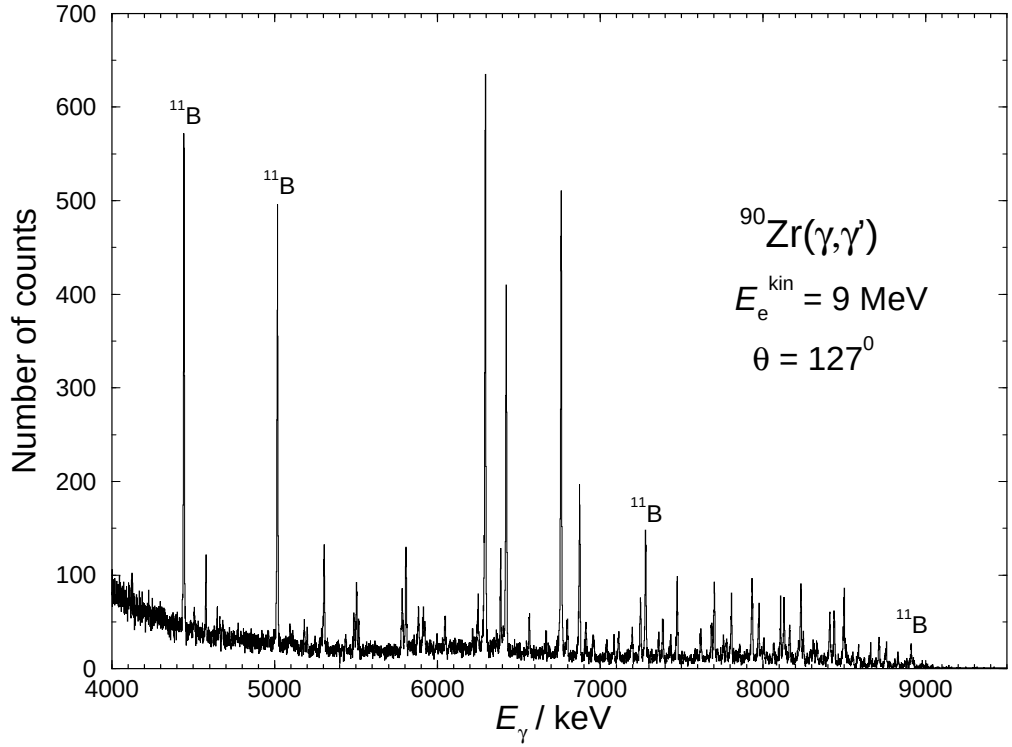

Summary

- Dipole-strength distributions of even-even Mo isotopes have been studied up to the respective neutron-separation energies at the photon-scattering facility of the ELBE accelerator.
- The $M1$ strength distributions up to $E_x < 4$ MeV fragment with increasing deformation, which is qualitatively described by deformed-RPA calculations.
- The total $E1$ strength above 5 MeV decreases with increasing N/Z of the Mo isotopes, which is reproduced by deformed-RPA predictions.
- The total $E1$ strength above 5 MeV increases with increasing N/Z for $N = 50$ isotones.
- The high level density above 5 MeV in connection with feeding by high-lying states and branchings to low-lying states require new techniques in order to reconstruct the original dipole-strength distributions.
- Simulations of the decay of excited levels deliver an estimate of the branchings. The reconstructed dipole-strength distributions fit the low-energy tails of the giant dipole resonances.

P-nuclei and the γ-process

- 35 p-nuclei from ^{74}Se to ^{196}Hg cannot be produced in the s- or r-processes.
- They are produced and destructed by the p- or γ-process at temperatures of $T \approx (2 - 3) \cdot 10^9$ K.
- The γ-process comprises (γ,n), (γ,p) and (γ,α) reactions starting from s- and r-process seed nuclei.
- Abundances of p-nuclei are 10 to 1000 times smaller than those of their neutron-rich isotopes - except for Mo and Ru.

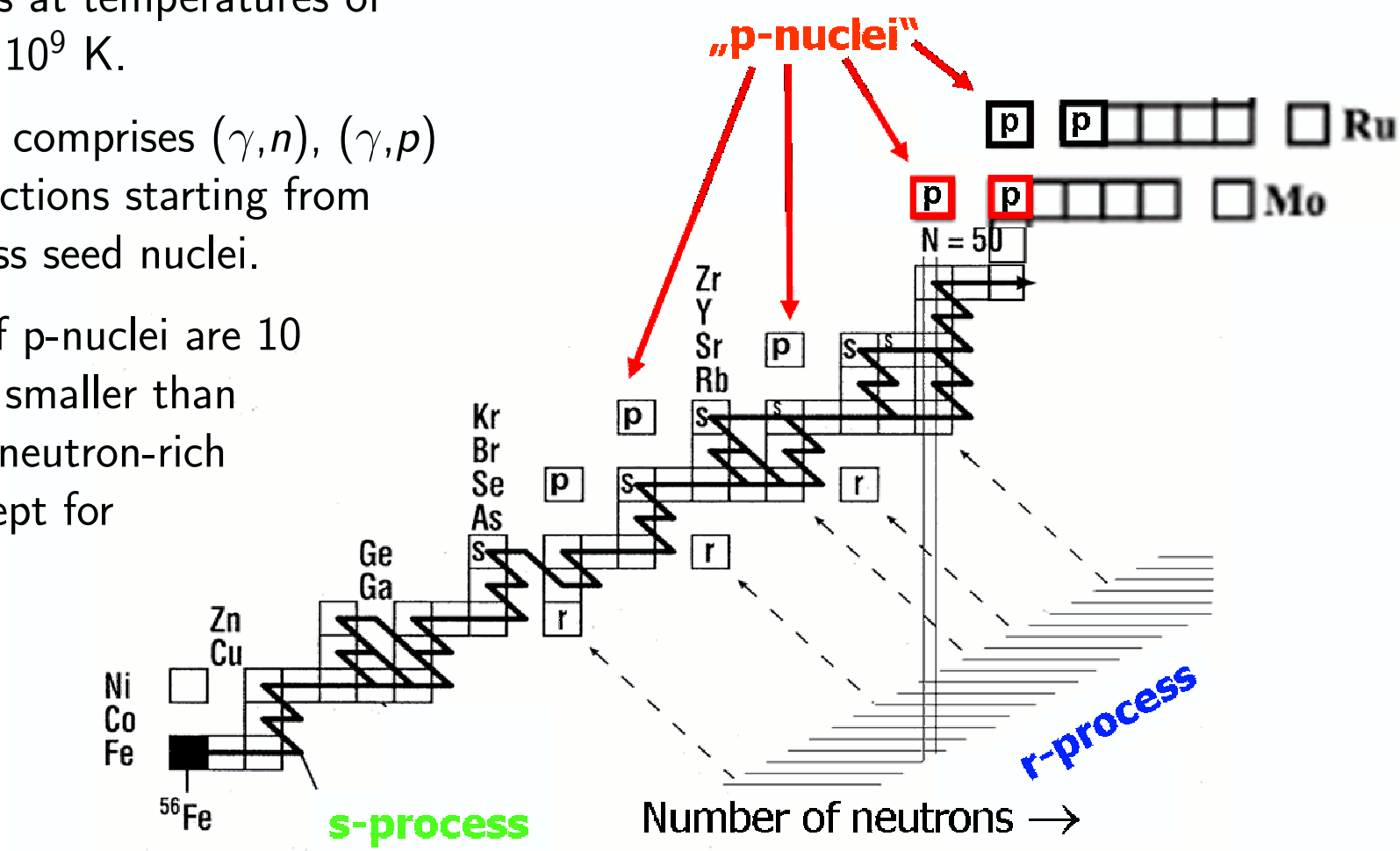

Calculation of abundances of p-nuclei

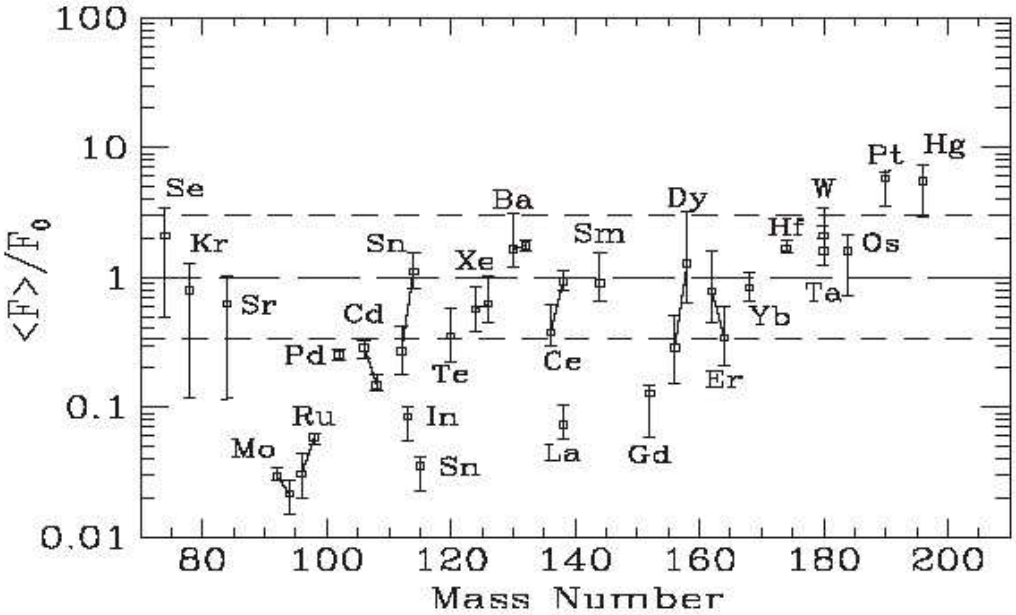

M. Arnould, S. Goriely,
PR 384 (2003) 1

- The abundances of Mo and Ru are underestimated by network calculations.
- Are the reaction rates correct?

⇒ Study of the photodissociation of ^{92}Mo

Setup for photoactivation experiments

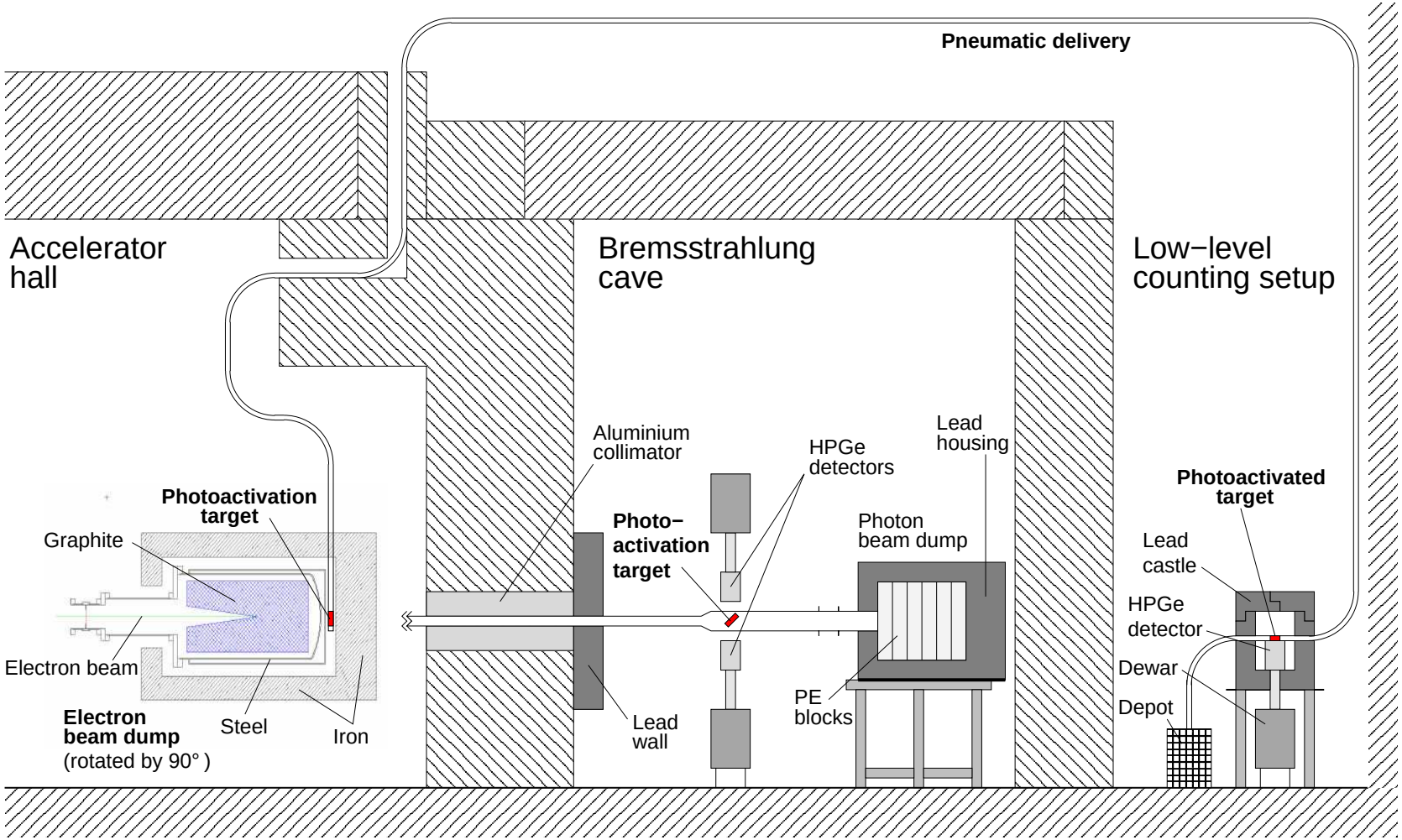

Photoactivation of ^{92}Mo

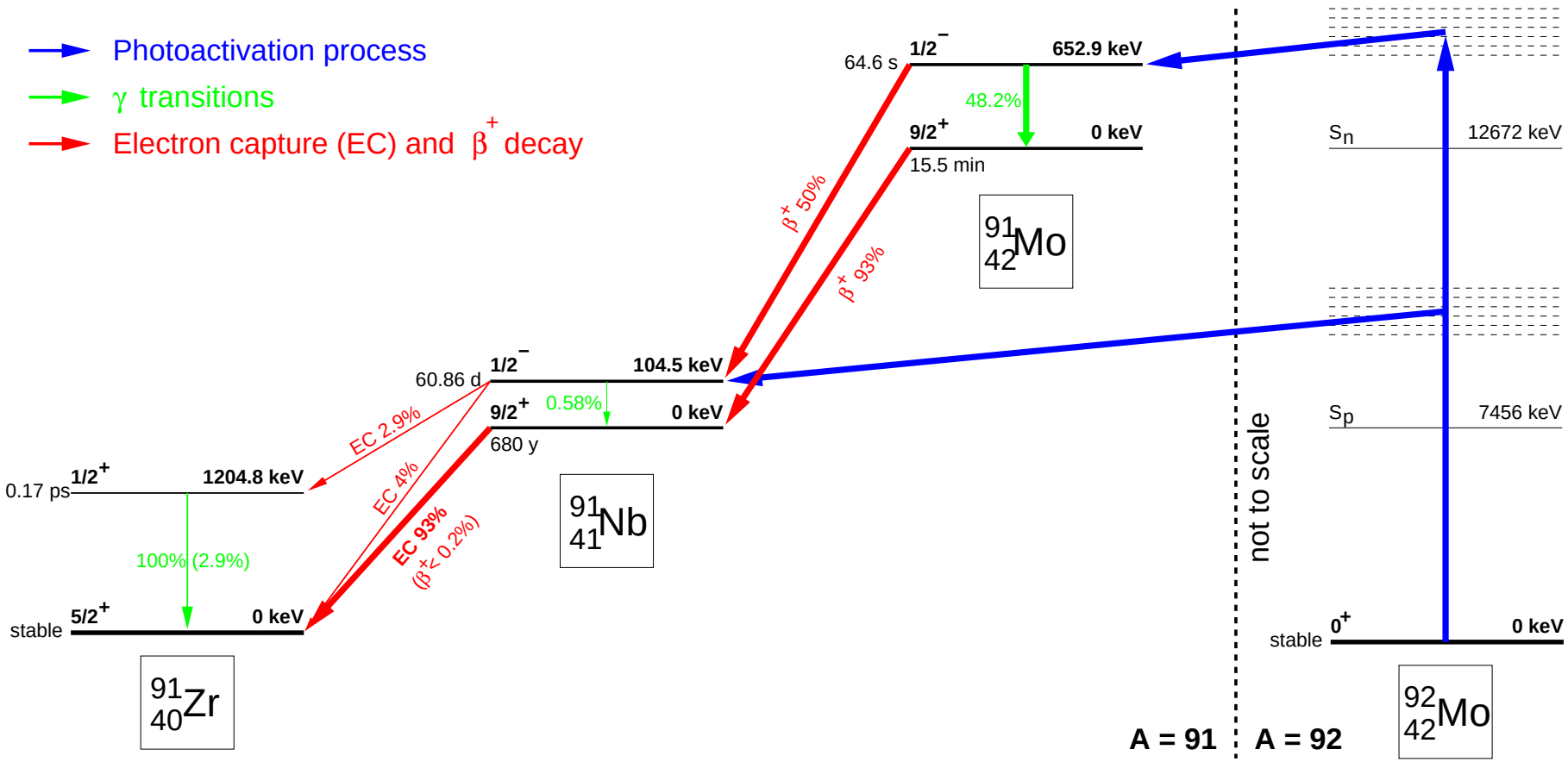

$$N_{\mathrm{act}}(E_{\mathrm{e}}) = N_{\mathrm{tar}} \cdot \int_{E_{\mathrm{thr}}}^{E_{\mathrm{e}}} \sigma_{(\gamma,x)} \; \Phi_{\gamma}(E, E_{\mathrm{e}}) \; dE$$

$$N_{\mathrm{act}}(E_{\mathrm{e}}) = I_{\gamma}(E_{\gamma}) \cdot \varepsilon^{-1}(E_{\gamma}) \cdot p^{-1}(E_{\gamma}) \cdot \kappa_{\mathrm{corr}}$$

Activation yield

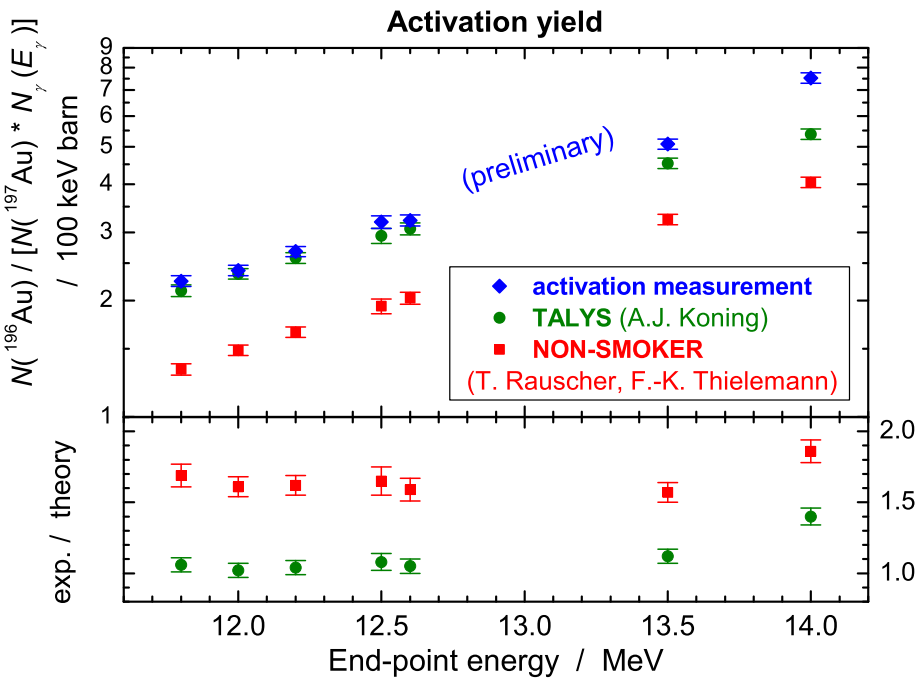

Activation yield of the $^{197}Au(\gamma, n)$ reaction. The yield is normalised to the number of ^{197}Au atoms and to the absolute photon flux at $E_\gamma = 8917$ keV.

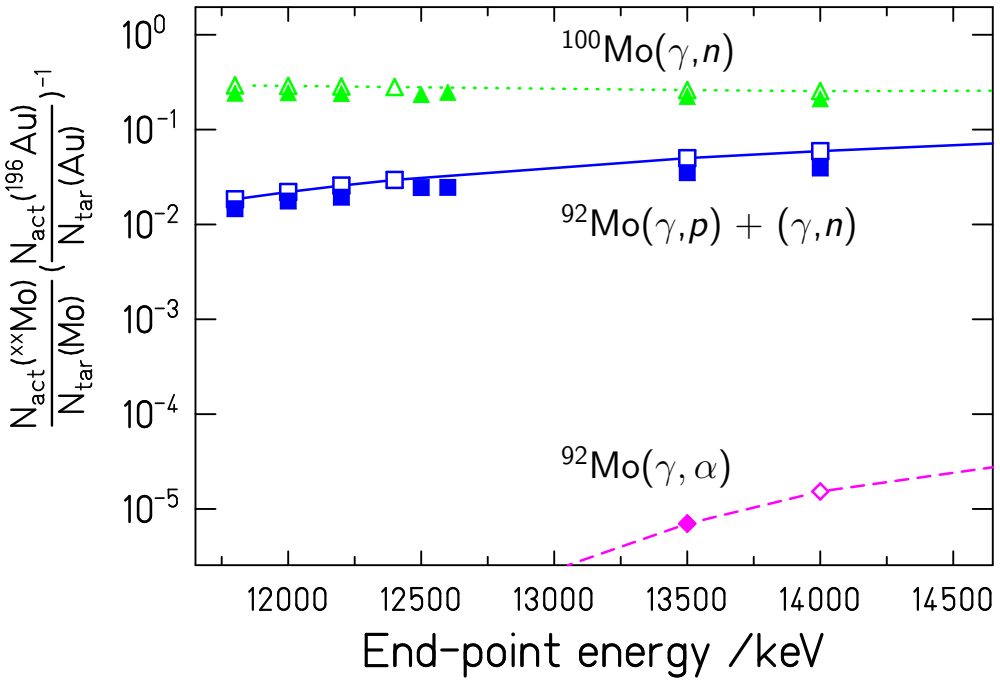

Activation yields of Mo isotopes normalised to the activation yield of the $^{197}Au(\gamma, n)$ reaction.

Open symbols:
T. Rauscher and F.-K. Thielemann,
ADNDT 88 (2004) 1

Summary

- Endpoint energy derived from the photodissociation of ^{2}H.
- Photon-flux distribution deduced from photon scattering from states with known widths in ^{11}B.
- Determination of the photon flux in the electron-beam dump by means of gold targets.
- Determination of the activation yield of the ^{92}Mo$(\gamma, p)^{91m}$Nb reaction up to $S_n(^{92}\mathrm{Mo})$ via the decay ^{91m}Nb(EC) $\rightarrow$ ^{91}Zr ($E_\gamma = 1205$ keV).
- Good agreement of the activation yield with theoretical predictions.
- ^{92}Mo$(\gamma, \alpha)^{88}$Zr observed for the first time.